Experimental and Numerical Investigation on 2-D Wing-Ground Interference

by

A K Kartigesh A/L Kalai Chelven

Dissertation submitted in partial fulfilment of
The requirements for the
Bachelor of Engineering (Hons)
(Mechanical Engineering)

JANUARY 2009

Universiti Teknologi PETRONAS
Bandar Seri Iskandar
31750 Tronoh
Perak Darul Ridzuan

CERTIFICATION OF APPROVAL

Experimental and Numerical Investigation on 2-D Wing-Ground Interference

by

A K Kartigesh A/L Kalai Chelven

A project dissertation submitted to the
Mechanical Engineering Programme
Universiti Teknologi PETRONAS
in partial fulfilment of the requirement for the
BACHELOR OF ENGINEERING (Hons)
(MECHANICAL ENGINEERING)

Approved by,

(AP Dr Hussain H. Al-Kayiem)

UNIVERSITI TEKNOLOGI PETRONAS

TRONOH, PERAK

January 2009

CERTIFICATION OF ORIGINALITY

This is to certify that I am responsible for the work submitted in this project, that the original work is my own except as specified in the references and acknowledgements, and that the original work contained herein have not been undertaken or done by unspecified sources or persons.

A K KARTIGESH A / L KALAI CHELVEN

ABSTRACT

The wing collision is a practical aerodynamic problem. All aerodynamics characteristic of the wing are changing in the collision phenomena. In the present project, the collision of 2-D airfoil section with ground will be investigated experimentally and numerically. The study includes a series of wind tunnel experiments to investigate the 2-D wing influence under collision. Numerical simulation by CFD has been carried out using FLUENT software in order to identify the changes of aerodynamics characteristics during the wing collision. The 2-D wing section selected for the study is NACA 4412 airfoil. The investigation has been carried out at different Reynolds Number ranging from (0.1×10^6 to 0.4×10^6), different angles of attack (-4^0 to 20^0) and different height above the ground.

Based on take off and landing fly stages the boundary conditions for the experimental and numerical analysis are determined. An experimental set up was designed and constructed to simulate the collision phenomena in a subsonic wind tunnel. The results of the airfoil characteristic are presented in non-dimensional form as lift, drag and pitching moment coefficient.

ACKNOWLEDGEMENT

My sincere appreciation goes to Universti Teknologi PETRONAS (UTP) and all individuals that have contributed to the continued development and refinement of this dissertation of Final Year Project (FYP) in order to complete my partial fulfillment of the requirement for the Bachelor of Engineering (Hons) Mechanical Engineering.

My special thanks to my supervisor, Assoc. Prof. Dr. Hussain H. Al-Kayiem for his supervision and his confidence in me through out this project. Also for his tremendous support, advices, and information. Thanks to lab Technician, Mr. Zailan for his comments, advices and technical assistance.

Last but not least, thank you for those who are contributed directly and indirectly to the success of this project. Special recognition to my beloved family, father - Kalai Chelven, mother - Periyanayaki, Sister - Sumathi for their endless love and support through thick and thin in leading life.

TABLE OF CONTENTS

CERTIFICATION OF APPROVAL			i
CERTIFICATION OF ORIGINALITY			ii
ABSTRACT			iii
ACKNOWLEDGEMENT			iv
TABLE OF CONTENTS			v
LIST OF FIGURES AND TABLES			vi
NOMENCLATURE			viii
CHAPTER 1:	**INTRODUCTION**		1
	1.1	Background of Study	1
	1.2	Problem Statement	3
	1.3	Objectives and Scope of Study	3
	1.4	Scope of study	3
CHAPTER 2:	**LITERATURE REVIEW AND THEORY.**		4
	2.1	Literature Survey	4
	2.1	Principle of Ground Effect.	5
	2.2	Theory	8
CHAPTER 3:	**METHODOLOGY**		13
	3.1	Analysis Method	13
	3.2	Project Flow Chart	13
	3.3	Gantt Chart	16
CHAPTER 4:	**RESULTS AND DISCUSSION.**		17
	4.1	Phase 1(NACA 4412 Coordinates).	17
	4.2	Phase 2(Experimental).	21
	4.3	Phase 3(Simulation)	29
	4.4	Discussion	48
CHAPTER 5:	**CONCLUSION AND RECOMMENDATION**		49
	5.1	Conclusion	49
	5.2	Recommendation	50
REFERENCES			51
APPENDICES			53

APPENDIX A: AIRFOIL MODELS. 53

APPENDIX B: FUNDAMENTAL FLUID MECHANICS . 53

LIST OF FIGURES AND TABLES

Figure 1.1: Phenomena of ground effect 1

Figure 2.1: Wingtip Sketch 5

Figure 2.2: Airfoil Sketch subjected to airstreams 6

Figure 2.3: Graph of normal induced drag against % of wingspan . . 7

Figure 2.4: Effective Span 10

Figure 2.5: CFD Results 11

Figure 2.6: Boundary Condition for Airfoil modeling in ground effect . 12

Figure 3.1: Project Flow Chart 15

Figure 3.2: Gantt chart 16

Figure 4.1: Naca 4412 Model Cconstructed using the Laser Digitizer Data . 17

Figure 4.2: 100 Coordinate points of Naca 4412 Model . . . 18

Figure 4.3: Critical Zone for Experimental Analysis . . . 21

Figure 4.4: Experimental Arrangement 22

Figure 4.5: Subsonic Wind Tunnel 22

Figure 4.6: NACA 4412 Airfoil Model 23

Figure 4.7: Test section floor as ground 23

Figure 4.8: Sample arrangement of the airfoil closer to the ground . . 24

Figure 4.9: Graph of AOA against Coefficient of Lift, Drag and Moment . 25

Figure 4.10: Graph of Re Number against Coefficient of Lift and Drag . 26

Figure 4.11: Graph of Re Number against Coefficient of Pitching Moment . 27

Figure 4.12: Graph of H/C Ratio against Coefficient of Lift and Drag . 28

Figure 4.13: NACA 4412 Vertexes plotted on GAMBIT . . . 29

Figure 4.14: NACA 4412 Edges plotted on GAMBIT . . . 29

Figure 4.15: Boundary Model 30

Figure 4.16: Boundary Model for H/C= 0.1 and angle of attack $\alpha = 0^{o}$. 31

Figure 4.17: Boundaries applied in GAMBIT . . . 32

Figure 4.18: Stretched meshing of the flow field 32

Figure 4.19: Pressure Coefficient against the position . . . 33
Figure 4.20: Contour of static pressure around the Airfoil . . . 34
Figure 4.21: Contour of dynamic pressure around the Airfoil . . 35
Figure 4.22: Contour of velocity magnitude around the Airfoil . . 36
Figure 4.23: CL vs AOA at H/C = 0.1, Re =0.4 e+6 37
Figure 4.24: CD vs AOA at H/C = 0.1, Re =0.4 e+6. 38
Figure 4.25: CM vs AOA at H/C = 0.1, Re =0.4 e+6 38
Figure 4.26: CL vs Re at AOA = 4, H/C = 0.1 39
Figure 4.27: CD vs Re at AOA = 4, H/C = 0.1 39
Figure 4.28: CM vs Re at AOA = 4, H/C = 0.1 40
Figure 4.29: CL vs H/C Ratio at different Re and AOA . . . 41
Figure 4.30: CD vs H/C Ratio at different Re and AOA . . . 41
Figure 4.31: Comparison Graph of H/C Ratio against CL and CD . . 42
Figure 4.32: Comparison of Experimental work with previous work . 44
Figure 4.33: Comparison of Simulation work with previous work . . 46
Figure A1: Airfoil Models 53
Table 2.1: Turbulence Flow for NACA 4412 in Ground Effect results . 4
Table 4.1: NACA 4412 Coordinates (published data) [10] . . . 19
Table 4.2: Comparison of coordinates 20
Table 4.3: Boundary conditions 21
Table 4.4: Angle of Attack against Coefficient of Lift, Drag and Moment . 24
Table 4.5: Reynolds Number against Coefficient of Lift, Drag and Moment 26
Table 4.6: Height to Chord Ratio against Coefficient of Lift and Drag . 27
Table 4.7: Angle Of Attack 33
Table 4.8: AOA against CL, CD, and CM 37
Table 4.9: Re against CL, CD, and CM 39
Table 4.10: H/C Ratio against CL and CD 40
Table 4.11: Error between the Experimental data and Simulation data . 43
Table 4.12: Error between Experimental work and previous work . . 45
Table 4.13: Error between Simulation work and previous work . . 47

NOMENCLATURE

NACA 4412	**Aircraft Wing Section Model**
CFD	**Computerized Fluid dynamics**
Re	**Reynolds Number**
α	**Angle of Attack**
ρ	**Density of Air**
μ	**Viscosity of Air**
V	**Fluid Velocity**
C_L	**Lift Coefficient**
C_M	**Moment Coefficient**
C_D	**Drag Coefficient**
C	**Chord Length**
L	**Lift Force**
M	**Pitching Moment**
D	**Drag Force**
H	**Height (between the Chord Line and the Ground)**
S	**Projected Area**
L / D	**Lift to Drag Ratio**
H / C	**Height to Chord Ratio**
SDGE	**Span Dominated Ground Effect**
CDGE	**Chord Dominated Ground Effect**
B or b	**Span**
H / B	**Height to Span Ratio**
B^2 / S	**Geometric Aspect Ratio**
X_p	**Centre of Pressure**
e	**Span efficiency**
AR	**Aspect Ratio**
AOA	**Angle of Attack**

CHAPTER 1
INTRODUCTION

1.1 BACKGROUND

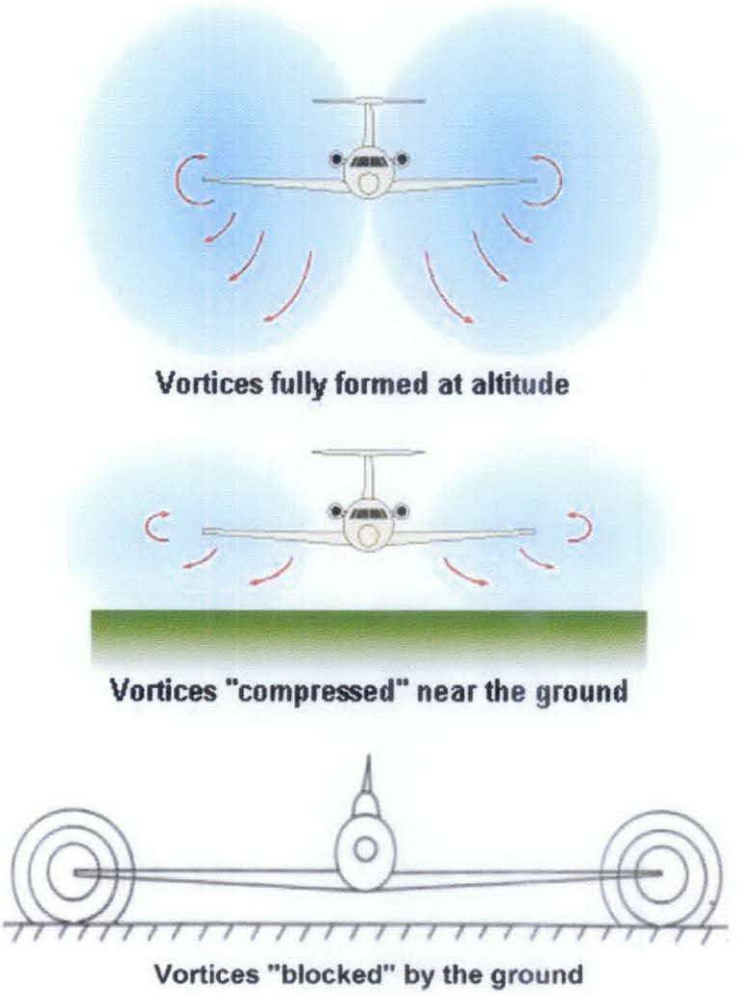

Figure 1.1: Phenomena of ground effect [7]

Aircraft may affected by a number of aerodynamics effects and ground effects due to a flying body's proximity to the ground. One of the most practical problems is the wing ground interference/wing in ground effect, or what is called collision during take off and landing of aircrafts.

The aerodynamic characteristics of wing are changing in the collision phenomena. That refers to the lift force experienced by an aircraft as it approaches a height approximately twice the chord length off the ground. The lift force increases as the wing moves closer the ground, with the most significant effects occurring at a height of one tenth of height to chord ratio. It shows that there is a potential hazard for inexperienced pilots who are not accustomed to adjusting for it on their way to take off and landing.

In order to investigate the aerodynamic characteristics of aircraft wings during take off and landing (wing ground interference) an airfoil model was selected. Airfoil, NACA 4412 was selected as the shape of the body for the experiments in the wind tunnel and CFD analysis. This 2-D section was introduced by Abot and Von Doenhoff (1959) and also by Ladson and Brooks Jr.(1975) with the purpose of airfoil geometries could be easily studied[1].

In both the experiments and simulation, angle of attack (α) and Reynolds Number (RE) became the main character to be tested. Angle of attack was described as" the angle at which the wing is inclined relative to the air flow"(Barnard and. Philpot,1995) [2]. Reynolds Number is usually used to identify and predict different flow regimes, such as laminar or turbulent flow.Adjustment to these main characters woul lead to spectacular change in lift, C_L, drag, C_D, pitching moment, C_M.For NACA 4412, it is catergorized as high lift wing.

CFD analysis has become the most powerful tool to stimulate the aerodynamic characteristic of an airfoil wing section. By using CFD analysis, the aerodynamic characteristics of the 2-D wing can be stimulated and numerically analyzed during the take off and landing which related to the wing ground interference and proved by the experiment that will be conducted in a low speed wind tunnel using the airfoil, NACA 4412 model.

1.2 PROBLEM STATEMENT

The wing ground interference, or what is called collision, is a practical problem during take off and landing of aircrafts. All the aerodynamics characteristics of wing are changing dramatically in the collision phenomena. Pilots often describe a feeling of "floating" or "riding on a cushion of air" that forms between the wing and the ground. The effect of this behavior is the sudden increase in lift of the wing and makes it more difficult for the pilots to the approach of landing and take off. Experimental and numerical investigations on a 2-D wing-ground interference are to be carried out to analyze the problem.

1.3 OBJECTIVES

- To conduct a series of wind tunnel experiments to investigate the 2-D,NACA 4412 airfoil section Influence under collision.
- Simulate (CFD) and analyze numerically the wing during take off and landing using FLUENT.

1.4 SCOPE OF STUDY

The wing collision is a practical aerodynamic problem. In this project, the collision of 2-D airfoil section with ground will be investigated experimentally and numerically.

- The experiments are to be conducted in low speed wind tunnel using the airfoil NACA 4412. The process of preparing the wing-ground interference model in the wind tunnel for the experiment will be part of the scope of study.
- The numerical simulation is to be carried out using FLUENT software. Utilization of the software will be one of the major requirements for the project.
- These investigations will be carried out at different Reynolds Number and different angles of attack and at different heights above the ground.

CHAPTER 2

LIERATURE REVIEW AND THEORY

2.1 LITERATURE SURVEY

In the year 2000, Zhang and Jonathan have conducted experimental and numerical analysis on Turbulent Wake behind a Single Element Wing in Ground Effect.
As the ground height is reduced, boundary layer separation occurs on the suction surface. The size of the turbulent wake grows. This has a turning effect on the wake, such that as the wake develops, it comes closer to the ground. [3]

In the year 2006, Firooz and Gadami have conducted computational analysis on the Turbulence Flow for NACA 4412 in Unbounded Flow and Ground Effect. [4]

Table 2.1: Turbulence Flow for NACA 4412 in Ground Effect results [4]

H/C	*CL*		*CD*10*		*Cf*100*		*Cp*100*	
	moving	*fixed*	*moving*	*fixed*	*moving*	*fixed*	*moving*	*fixed*
0.08	1.2934	1.171	0.12144	0.1304	0.61594	0.6889	0.59843	0.61514
0.1	1.2603	1.1791	0.1219	0.12566	0.63744	0.6855	0.58183	0.57097
0.2	1.1674	1.156	0.12518	0.11969	0.7022	0.7167	0.5495	0.48012
0.3	1.1241	1.1271	0.13209	0.12344	0.75362	0.7619	0.56723	0.4722
0.5	1.0975	1.1064	0.13474	0.12518	0.78268	0.7877	0.5952	0.464
0.8	1.093	1.1017	0.14052	0.13139	0.807	0.80766	0.60022	0.50685
∞	1.0848		0.1815		0. 8576		0.9575	

Nathan Logsdon, 2006 has done a study on airfoils and wing sections he prepared a procedure for numerically analyzing airfoils and wing sections. GAMBIT is modeling software that is capable of creating meshed geometries that can be read into FLUENT and other analysis software. [5]

Heffley, 2007 has conducted a series of wind tunnel experiments using NACA 4412 Airfoil model to determine the Aerodynamic Characteristics during low speed wind flow through the model. Lift coefficient agrees within 2% of NACA published data. Noticeable inaccuracies in drag coefficient data from the pressure ported airfoil Drag coefficient is Re dependent. [6]

2.2 PRINCIPLES OF GROUND EFFECT

To understand what ground effect is and how it functions, we first need to take a step back and explain some aerodynamic properties of an airplane wing. When producing lift, a wing generates strong swirling masses of air off both its wingtips. As discussed in a previous question on the creation of lift, a wing generates lift because there is a lower pressure on its upper surface than on its lower surface. This difference in pressure creates lift, but the penalty is that the higher pressure flow beneath the wing tries to flow around the wingtip to the lower pressure region above the wing. This motion creates what is called a wingtip vortex. As the wing moves forward, this vortex remains, and therefore trails behind the wing. For this reason, the vortex is usually referred to as a trailing vortex. One trailing vortex is created off each wingtip, and they spin in opposite directions as illustrated below. [7]

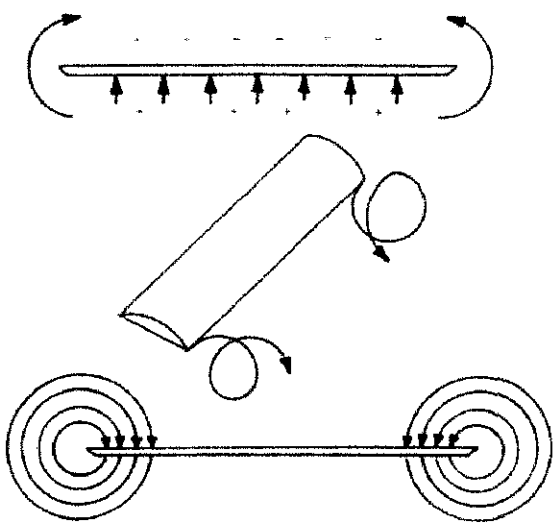

Figure 2.1: wingtip sketch [7]

Besides generating lift the trailing vortices also has their primary effect that deflecting the flow behind the wing downward. This induced component of velocity is called downwash, and it reduces the amount of lift produced by the wing. In order to make up for that lost lift, the wing must go to a higher angle of attack, and this increase in angle of attack increases the drag generated by the wing. We call this form of drag induced drag because it is "induced" by the process of creating lift.

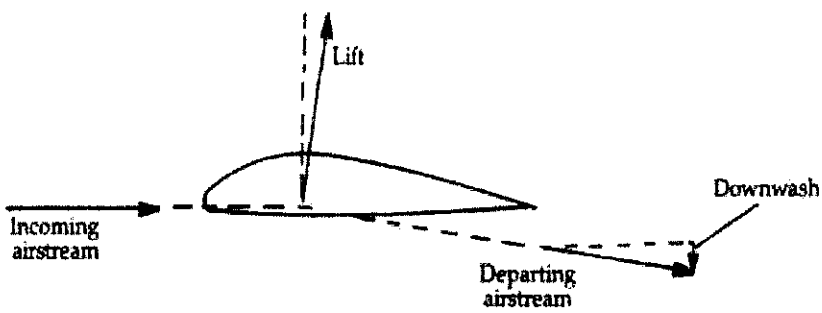

Figure 2.2: Airfoil sketch subjected to airstreams [7]

The phenomenon is most often observed when an airplane is landing, and pilots often describe a feeling of "floating" or "riding on a cushion of air" that forms between the wing and the ground. The effect of this behavior is to increase the lift of the wing and make it more difficult to land.

However, there is no "cushion of air" holding the plane up and making it "float." What happens in reality is that the ground partially blocks the trailing vortices and decreases the amount of downwash generated by the wing. This reduction in downwash increases the effective angle of attack of the wing so that it creates more lift than it would otherwise. This phenomenon is the wing in ground effect. [7]

Ground effect that becomes more significant as speed increases is called ram pressure. As the distance between the wing and ground decreases, the incoming air is "rammed" in between the two surfaces and becomes more compressed. This effect increases the pressure on the lower surface of the wing to create additional lift.

The impact of ground effect increases the closer to the ground that a wing operates. As indicated in the plot shown in figure 2.5, ground effect typically does not exist when a plane operates more than one wingspan above the surface. At an altitude of 1/10 wingspan but induced drag is decreased by half. [7]

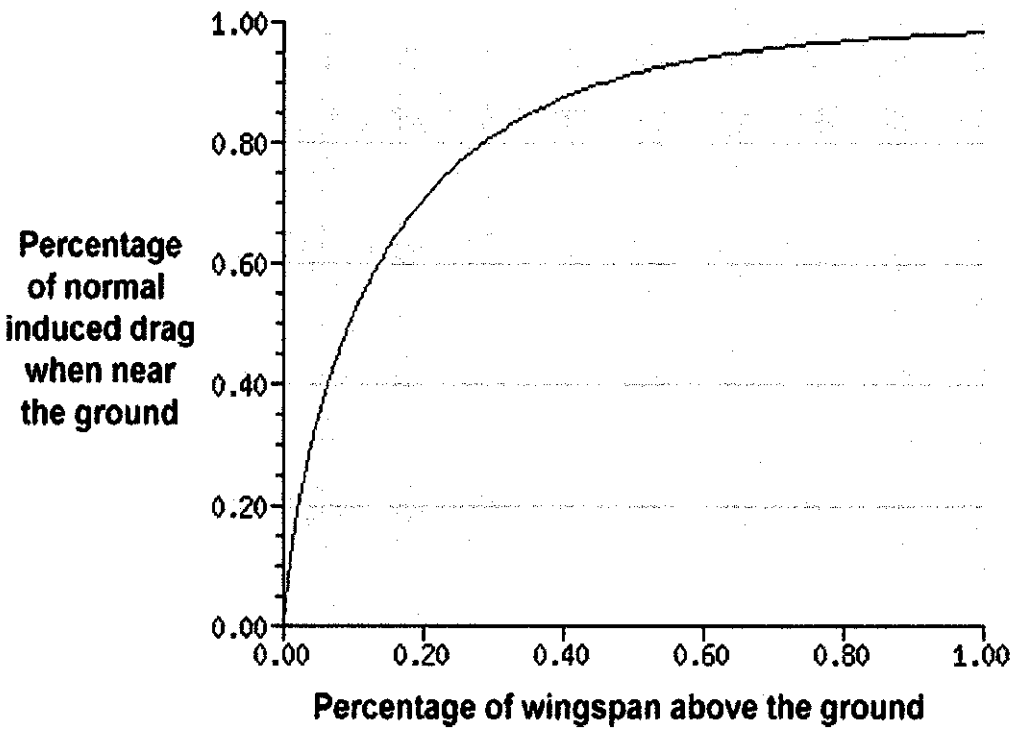

Figure 2.3: Graph of normal induced drag against % of wingspan [7]

A vehicle operating in ground effect has the potential to be much more efficient than an aircraft operating at high altitude. The aerodynamic efficiency of an aircraft is expressed through a quantity called the lift-to-drag ratio, or L/D.

Typical L/D values for conventional, subsonic aircraft are on the order of 15 to 20. By comparison, a ground effect vehicle could, in theory, achieve L/D ratios closer to 25 or 30. [7]

2.2 THEORY

When a wing approaches the ground, an increase in lift as well as a reduction in drag is observed which results in an overall increase in the lift-to-drag ratio. The cause of the increase in lift is normally referred to as chord dominated ground effect (CDGE) or the ram effect. Meanwhile, the span dominated ground effect (SDGE) is responsible for the reduction in drag. The combination of both CDGE and SDGE will lead to an increase in the L/D ratio hence efficiency increases.

In the study of CDGE, one of the main parameters which one considers is the height-to chord (H/C) ratio, H. The term height here refers to the clearance between the ground surface and the airfoil or the wing. The increased in lift is mainly because the increased static pressure creates an air cushion when the height decreases. This result in a ramming effect whereby the static pressure on the bottom surface of the wing is increased, leading to higher lift. Theoretically, as the height approaches 0, the air will become stagnant hence resulting in the highest possible static pressure with a unity value of coefficient of pressure. [8]

Following the convention of the study of aerodynamics, the solutions of the aerodynamic forces, Lift (L) and Drag (D), and moment (M) are normally presented in a form of dimensionless coefficient which are define as the following:

$$C_L = L / 0.5\, \rho\, V^2\, S$$

$$C_D = D / 0.5\, \rho\, V^2\, S$$

$$C_M = M / 0.5\, \rho\, V^2\, S$$

where p is density of air, S is projected area on ground plane, V is free stream velocity and c is the chord length.

It has predicted for a case a flat plate with infinite span in the presence of extreme ground effect (H/C < 10%), a closed form solution for C_L and C_M can be obtained by a modification to the thin airfoil theory and the solutions are given as:

$$C_L = \alpha / H$$

$$C_M = -\alpha / 3H$$

In the previous equation, the coefficient of moment is taken with respect to the leading edge. By taking the moment at the leading edge, the center of pressure, x_p is:

$$x_p = C_M / C_L = -1 / 3$$

Hence unlike the case of a symmetrical airfoil out of ground effect, the center of pressure is at one-third of the cord instead of one-forth. Coincidentally, for a symmetrical airfoil, the center of pressure coincides with the aerodynamic center. This is however not true for a cambered airfoil.

On the other hand, the study of SDGE consists of another parameter known as the height to- span (h/b) ratio. The total drag force is the sum of two contributions" profile drag and induced drag. The profile drag is due to the skin friction and flow separation. Secondly, the induced drag occurs in finite wings when there is a 'leakage' at the wing tip which creates the vortices that decreases the efficiency of the wing. In SDGE, the induced drag actually decreases as the strength of the vortex is now bounded by the ground. As the strength of the vortex decreases, the wing now seems to have a higher effective aspect ratio as compared to its geometric aspect ratio (b^2/S) resulting in a reduction in induced drag. [8]

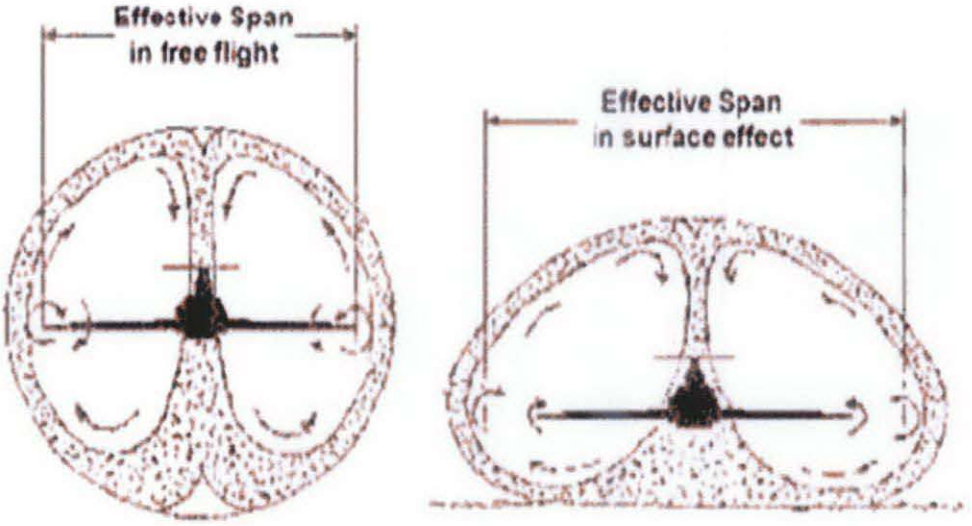

Figure 2.4: Effective Span [8]

From Prandtl's lifting line theory, the induced drag can be calculated by

$$C_D = C_L^2 / \pi e AR$$

where e is known as the span efficiency and AR is the aspect ratio. In the presence of ground effect, shows that

e directly proportional to 1 / H

C_D directly proportional to H

It shows that the induced drag will decrease linearly with height.

CFD Analysis

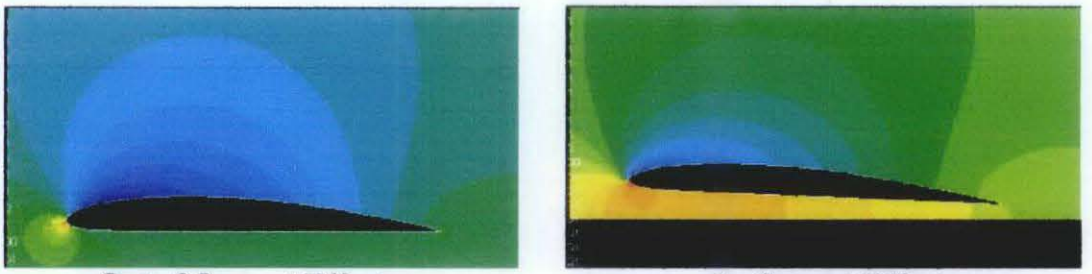

Out of Ground Effect **In Ground Effect**

Figure 2.6: CFD Results [8]

In the study of aerodynamics, whether it is theoretical, experimental or computational, all efforts are normally aimed at one objective: To determine the aerodynamic forces and moments acting on a body moving through air. The main purpose of employing CFD here is to predict and obtain these aerodynamic forces, Lift and Drag, and Moments, acting on the craft so that the data can be use for design and analyses for later stage of the project.

Another advantage of using CFD is its ability to perform flow visualization. Air being invisible, under normal circumstances, the human's naked eye is unable to see how the air behaves. Typically, flow visualization is being carried out either in a smoke tunnel or water tunnel. But with CFD, flow can be visualize by analyzing the velocity vector plots and injecting tracking the particles being injected into the simulation and by observing the flow pattern will enable a better understanding of the physics of the flow.

Existing analytical solution for airfoils and wings that are developed were based on the assumption of in viscid flow. Those methods are fairly accurate if the operating Reynolds's number (Re) base on the free stream velocity and the chord length is very high. From the Thin Airfoil Theory, the coefficient of lift is proportional to the angle of attack and independent of the free stream velocity.[8]

$$\mathbf{Re = \rho . V . C / \mu}$$

where C = Chord length, ρ = air density, μ = air viscosity, V = air velocity

Boundary Conditions used for Airfoil Modeling considering the Ground Effect

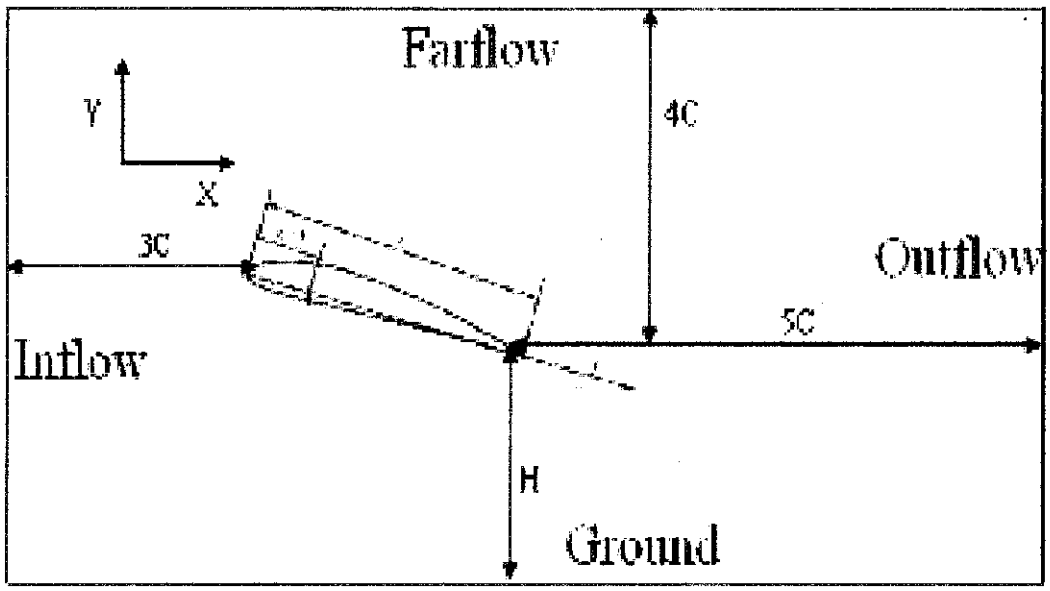

Figure 2.6: Boundary Condition for Airfoil modeling in ground effect [8]

Distance from the ground is determined based on the chord length and consider the ratio of H/C (Ground /Chord Length).The ratio H/C will usually Varies from 0.08 to 0.8/1.0.(8%-100%).Based on the literature survey, the critical zone is when the ratio H/C < 10%. As the airfoil approaches the ground, the pressure on the pressure side of the airfoil gradually increases due to the slow-down of the flow, resulting in a large lift increase.

Therefore the most extreme and effective distance from the Airfoil to the ground would H/C < 10% so that the aerodynamics characteristic can be effectively analyzed. [8]

CHAPTER 3
METHODOLOGY

The project started with some research based on books, journals, technical papers, thesis and articles obtained from various sources.Some consultation sessions were held with the supervisor and lecturers on the project overview.The following action plan will be collecting the Airfoil model which was previously manufactured. Some prelimanary works has to carry out before moving on to the real objectives of the project.

3.1 ANALYSIS METHOD

Based on the literature survey done, a basic knowledge on wing in ground phenomena is clearly studied. Thus the method of work will follow the 3 phase of the project.

Phase 1

1. Detect the surface of the NACA 4412 Airfoil using CNC Laser Digitizer.
2. Obtain the coordinates of the Airfoil from the Laser Digitizer
3. Compare the coordinates with the standard coordinates of the NACA 4412 Airfoil.
4. Estimate the percentage errors.

Phase 2

1. Experimental Investigation of the NACA 4412 Airfoil in a low speed wind tunnel.
2. Conduct the experiments for different conditions as listed below

    - Operate the wind tunnel without the airfoil to detect and set the zero errors of the reading.(include the carrier)
    - Perform the experiment with the NACA Airfoil for different angle of attack ($\alpha = -4^0$ to 20^0) and repeat at different Re number.
    - Create the experimental model inside the wind tunnel for ground effect analysis of the NACA 4412 Airfoil.
    - Perform the experiment again with the ground effect model and NACA 4412 Airfoil for different angle of attack and different Re number.

Phase 3

1. CFD Analysis

    - Create the NACA 4412 Airfoil model using GAMBIT software
    - Set the boundary conditions for ground effect analysis.
    - Simulate the phenomena using FLUENT Software and obtain the flow visualization, analyzed the data obtained.
    - Compare the experimental data and the numerical data obtained throughout the investigation.
    - Conclude the project.

3.3 FLOW CHART

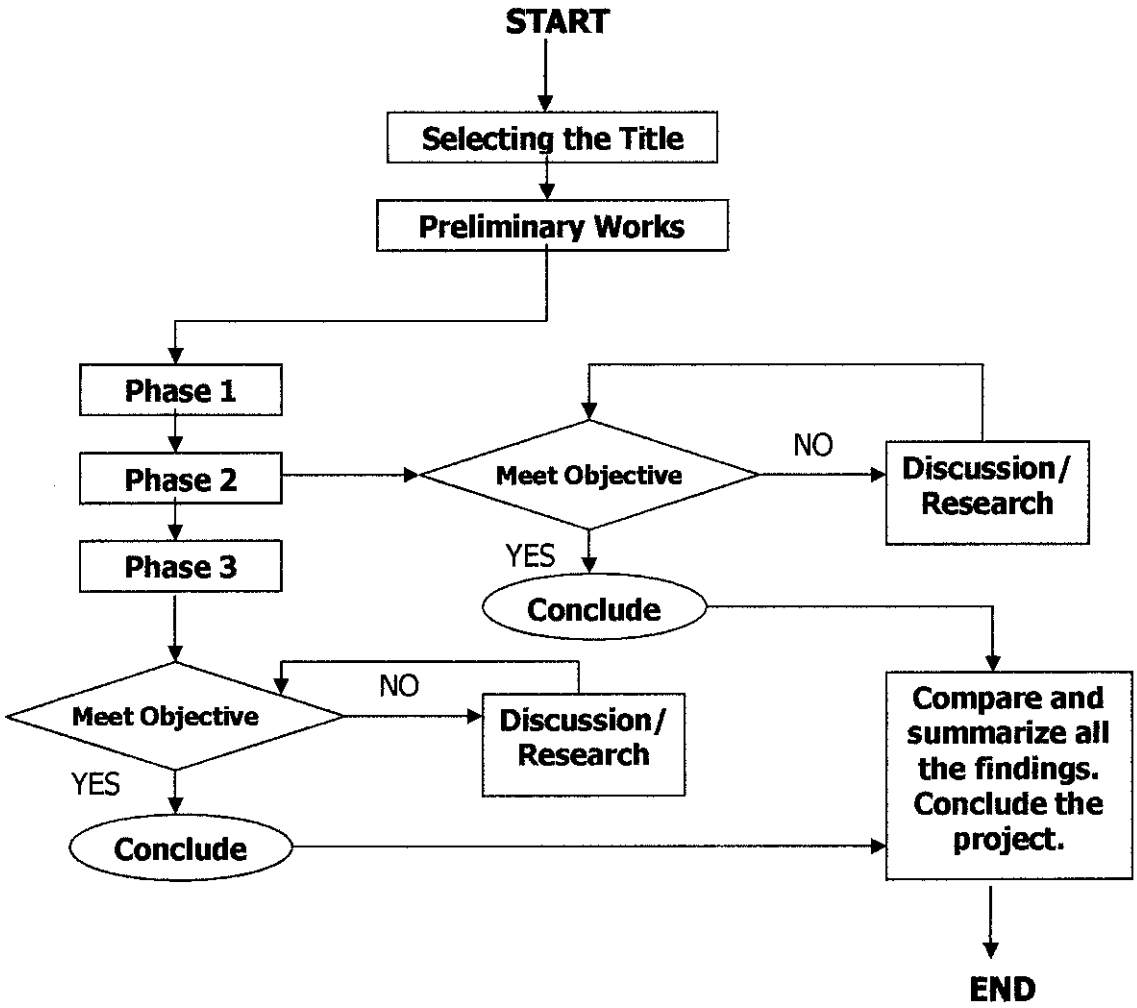

Figure 3.1: Project Flow Chart

Phase 1: Obtain Coordinates of NACA 4412 Airfoil Model

Phase 2: Wind Tunnel Experiments

Phase 3: Simulation (GAMBIT and FLUENT)

Meet Objective: Obtain the coefficients of lift, drag and pitching moment

Discussion / Research: Compare with published data.

3.2 GANTT CHART

Suggested Milestone for the First Semester of 2-Semester Final Year Project

No.	Detail / Week	1	2	3	4	5	6	7	8	9	10	11	12	13	14
1	Selection of Topic														
2	Preliminary Research Work														
3	Submission of Preliminary Report				•										
4	Search tools and Start Software tutorials														
5	Submission of Progress Report								•						
6	Seminar								•						
7	Project Work Continues														
8	Submission of Interim Report													•	
9	Oral presentation														•

• Suggested Milestones

Process

Suggested Milestone for the Second Semester of 2-Semester Final Year Project

No.	Detail / Week	1	2	3	4	5	6	7	8	9	10	11	12	13	14
1	Experimental and Simulation work continues														
2	Submission of Progress Report 1				•										
3	Experimental and Simulation work continues														
4	Submission of Progress Report 2								•						
5	Seminar								•						
6	Experimental and Simulation analysis work														
7	Poster Exibition										•				
8	Submission of Dissertation-Soft Bound												•		
9	Oral presentation													•	
10	Submission of Project Dissertation-Hard Bound														•

• Suggested Milestones

Process

Figure 3.2: Gantt chart

CHAPTER 4

RESULTS AND DISCUSSION

4.1 EXECUTION OF PHASE 1

4.1.1 Detect the surface of NACA 4412 model using Laser Digitizer

The surface of the NACA 4412 model is detected using the CNC Laser digitizer.The laser detection is projected to several surface of the model in order to obtained more accurate readings for the coordinates.The data file is saved and re-open the file using other software (FoilDesign) to display the coordinates. Below is the figure obtained by using the data on FoilDesign.

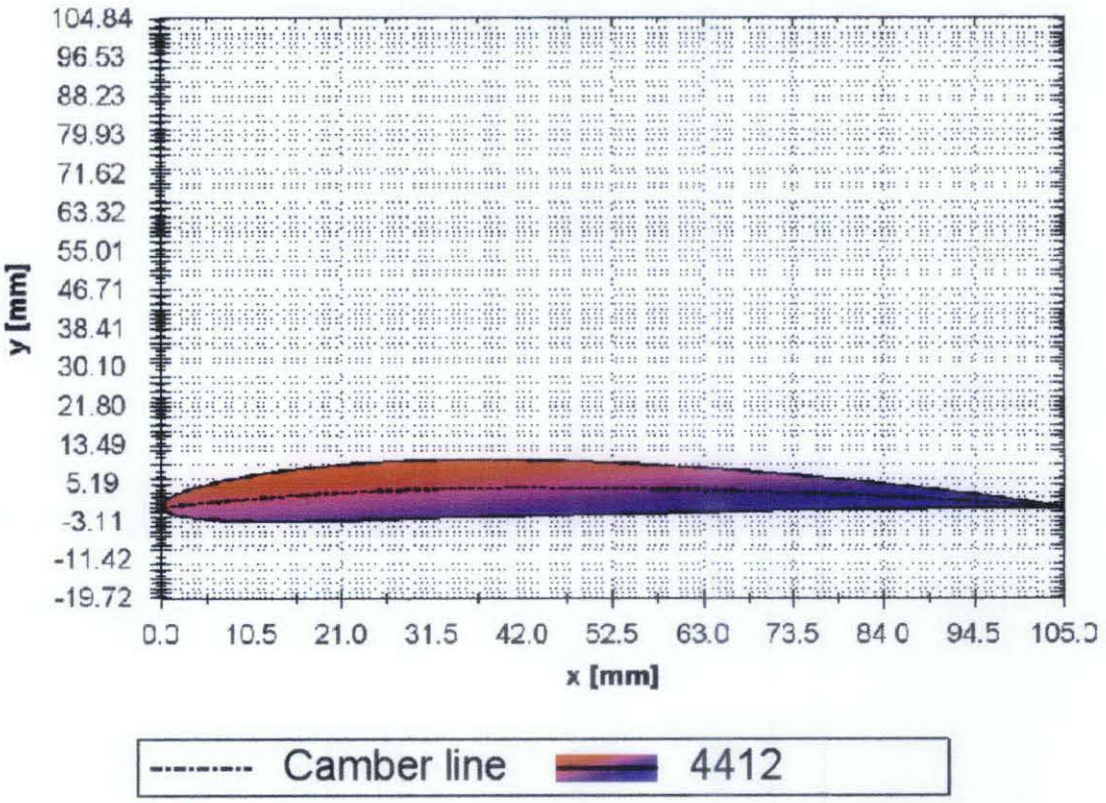

Figure 4.1: Naca 4412 Model Cconstructed using the Laser Digitizer Data

4.1.2 Generate the coordinates of the NACA 4412 model

After the model is constructed using the FoilDesign then we generate the coordinates of the Airfiol. Below are the coordinates obtain for NACA 4412 model.

NACA 4412 data 2.dat - Notepad

File Edit Format View Help

X	Yc	Xu	Yu	Xl	Yl
0	0	0	0	0	0
0.105	0.0207375	0.07076147	0.1963197	0.1392385	-0.1548447
0.21	0.04095	0.1637499	0.2843718	0.2562501	-0.2024718
0.315	0.0606375	0.2607507	0.3538768	0.3692493	-0.2326018
0.42	0.07979999	0.3599609	0.4133504	0.4800391	-0.2537504
0.525	0.0984375	0.4606605	0.4660922	0.5893396	-0.2692173
0.63	0.11655	0.5624681	0.5137967	0.6975319	-0.2806967
0.735	0.1341375	0.6651497	0.5574725	0.8048503	-0.2891975
0.84	0.1512	0.7685473	0.597779	0.9114527	-0.295379
0.9450001	0.1677375	0.872547	0.6351764	1.017453	-0.2997013
1.05	0.18375	0.9770623	0.670001	1.122938	-0.302501
1.155	0.1992375	1.082026	0.702509	1.227974	-0.3040339
1.26	0.2142	1.187382	0.7329004	1.332618	-0.3045005
1.365	0.2286375	1.293086	0.7613363	1.436914	-0.3040613
1.47	0.24255	1.399098	0.787948	1.540902	-0.302848
1.575	0.2559375	1.505387	0.8128453	1.644614	-0.3009703
1.68	0.2688	1.611921	0.836121	1.748079	-0.2985211
1.785	0.2811375	1.718678	0.8578547	1.851322	-0.2955798
1.89	0.29295	1.825632	0.8781154	1.954368	-0.2922154
1.995	0.3042375	1.932764	0.8969634	2.057236	-0.2884884
2.1	0.315	2.040055	0.9144522	2.159945	-0.2844522
2.205	0.3252375	2.147488	0.9306294	2.262512	-0.2801545
2.31	0.33495	2.255047	0.945538	2.364953	-0.275638
2.415	0.3441375	2.362718	0.9592164	2.467282	-0.2709415
2.52	0.3528	2.470488	0.9716999	2.569512	-0.2661
2.625	0.3609375	2.578344	0.9830208	2.671656	-0.2611458
2.73	0.36855	2.686274	0.9932084	2.773726	-0.2561084
2.835	0.3756375	2.794268	1.00229	2.875732	-0.2510152
2.94	0.3822	2.902314	1.010291	2.977685	-0.2458915
3.045	0.3882375	3.010405	1.017236	3.079595	-0.2407607
3.15	0.39375	3.11853	1.023145	3.18147	-0.235645
3.255	0.3987375	3.226681	1.02804	3.283319	-0.230565
3.36	0.4032	3.33485	1.03194	3.38515	-0.22554
3.465	0.4071375	3.44303	1.034863	3.486971	-0.2205881
3.57	0.41055	3.551212	1.036827	3.588788	-0.2157269
3.675	0.4134375	3.65939	1.037847	3.69061	-0.2109723
3.99	0.41895	3.983835	1.0354	3.996165	-0.1975001
4.095	0.4197375	4.091934	1.032795	4.098065	-0.1933197
4.2	0.42	4.2	1.029316	4.2	-0.1893161
4.305	0.4198833	4.306345	1.025128	4.303655	-0.1853618
4.41	0.4195333	4.41267	1.020395	4.40733	-0.1813283
4.515	0.41895	4.518974	1.015126	4.511025	-0.1772263
4.62	0.4181333	4.625255	1.009333	4.614745	-0.1730663
4.725	0.4170834	4.73151	1.003024	4.71849	-0.1688579
4.83	0.4158	4.837739	0.9962105	4.822261	-0.1646104
4.935	0.4142833	4.943938	0.9888995	4.926062	-0.1603328
5.04	0.4125333	5.050107	0.9811003	5.029892	-0.1560336
5.145	0.41055	5.156246	0.9728208	5.133755	-0.1517208
5.25	0.4083334	5.26235	0.9640688	5.23765	-0.1474021
5.355	0.4058833	5.368419	0.9548516	5.34158	-0.1430849
5.46	0.4032	5.474452	0.9451763	5.445547	-0.1387762
5.565	0.4002833	5.580449	0.9350494	5.549551	-0.1344828
5.67	0.3971333	5.686406	0.9244773	5.653594	-0.1302107
5.775	0.39375	5.792324	0.9134663	5.757676	-0.1259663
5.88	0.3901333	5.898201	0.9020218	5.8618	-0.1217551
5.985	0.3862833	6.004035	0.8901493	5.965965	-0.1175826
6.09	0.3822	6.109826	0.877854	6.070174	-0.1134541
6.195	0.3778833	6.215573	0.865141	6.174427	-0.1093743
6.3	0.3733333	6.321275	0.8520145	6.278726	-0.1053479
6.405	0.36855	6.42693	0.8384792	6.38307	-0.1013793
6.51	0.3635333	6.532538	0.8245392	6.487462	-0.09747247
6.615	0.3582833	6.638098	0.8101981	6.591902	-0.09363145
6.72	0.3528	6.743608	0.7954597	6.696392	-0.0898597
6.825	0.3470833	6.849069	0.7803274	6.800931	-0.08616072
6.93	0.3411333	6.954479	0.7648041	6.905521	-0.08253752
7.035	0.33495	7.059837	0.7488931	7.010163	-0.07899308
7.14	0.3285333	7.165142	0.7325968	7.114859	-0.07553012
7.245	0.3218833	7.270393	0.7159177	7.219607	-0.07215105
7.35	0.315	7.37559	0.6988582	7.324409	-0.06885813
7.455	0.3078834	7.480732	0.6814201	7.429267	-0.06565341
7.56	0.3005333	7.585819	0.6636053	7.534182	-0.06253868
7.665	0.29295	7.690848	0.6454155	7.639153	-0.05951556
7.77	0.2851333	7.795819	0.6268521	7.744181	-0.05658551
7.875	0.2770833	7.900731	0.6079164	7.849269	-0.05374966
7.98	0.2688	8.005585	0.5886091	7.954415	-0.05100907
8.085	0.2602834	8.110377	0.5689312	8.059622	-0.04836453
8.19	0.2515334	8.21511	0.5488834	8.16489	-0.04581665
8.295	0.24255	8.319779	0.5284658	8.270221	-0.04336583
8.400001	0.2333333	8.424386	0.507679	8.375614	-0.04101235
8.505	0.2238833	8.52893	0.4865229	8.481071	-0.03875621
8.61	0.2142	8.633408	0.4649973	8.586592	-0.03659729
8.715	0.2042834	8.73782	0.4431019	8.69218	-0.03453524
8.82	0.1941334	8.842166	0.4208363	8.797833	-0.03256954
8.925	0.18375	8.946445	0.3981994	8.903556	-0.03069949
9.03	0.1731333	9.050655	0.3751909	9.009345	-0.02892424
9.135	0.1622833	9.154795	0.3518094	9.115205	-0.02724271
9.24	0.1512	9.258864	0.3280537	9.221136	-0.02565367
9.345	0.1398834	9.362862	0.3039224	9.327138	-0.02415571
9.45	0.1283334	9.466786	0.279414	9.433213	-0.02274725
9.555	0.11655	9.570638	0.2545265	9.539363	-0.02142651
9.66	0.1045333	9.674413	0.2292582	9.645588	-0.02019159
9.765	0.09228333	9.778111	0.203607	9.751888	-0.01904038
9.87	0.0798	9.881732	0.1775706	9.858268	-0.0179706
9.974999	0.06708335	9.985274	0.1511465	9.964725	-0.01697982
10.08	0.05413336	10.08874	0.1243322	10.07126	-0.01606544
10.185	0.04094996	10.19212	0.0971246	10.17789	-0.01522467
10.29	0.02753331	10.29541	0.06952121	10.28459	-0.0144546
10.395	0.01388332	10.39862	0.04151876	10.39138	-0.01375211
10.5	0	10.50175	0.01311394	10.49825	-0.01311394

Figure 4.2: 100 Coordinate points of NACA 4412 Model

4.1.3 Published Data for NACA 4412 coordinates

Table 4.1: NACA 4412 Coordinates (published data) [10]

NACA 4412
(Stations and Ordinates gives in
percent of airfoil chord)

Upper surface		Lower surface	
Station	Ordinate	Station	Ordinate
0	0	0	0
1.25	2.44	1.25	-1.43
2.5	3.39	2.5	-1.95
5	4.73	5	-2.49
7.5	5.76	7.5	-2.74
10	6.59	10	-2.86
15	7.89	15	-2.88
20	8.8	20	-2.74
25	9.41	25	-2.5
30	9.76	30	-2.26
40	9.8	40	-1.8
50	9.19	50	-1.4
60	8.14	60	-1
70	6.69	70	-0.65
80	4.89	80	-0.39
90	2.71	90	-0.22
95	1.47	95	-0.16
100	0.13	100	-0.13
100	.....	100	0

Comparing the generated coordinates with published data

Choose 10 coordinates for comparison

Table 4.2: Comparison of coordinates

Upper surface			
Station	Published Ordinate	Generated Ordinate	% error
1.05	0.69195	0.67	-3
2.1	0.924	0.91445	-1
3.15	1.0248	1.023145	-0.16
4.2	1.029	1.029316	-0.03
5.25	0.96495	0.9640688	-0.09
6.3	0.8547	0.8520145	-0.3
7.35	0.70245	0.6988582	-1.2
8.4	0.51345	0.507679	-1.1
9.45	0.28455	0.279414	-0.005
10.5	0.01365	0.01311394	-0.17

Lower surface			
Station	Published Ordinate	Generated Ordinate	% error
1.05	-0.3003	-0.3025	-0.73
2.1	-0.28877	-0.28445	-1.5
3.15	-0.2373	-0.235645	-0.7
4.2	-0.189	-0.1893161	0.16
5.25	-0.147	-0.1474021	0.27
6.3	-0.105	-0.105348	0.33
7.35	-0.06825	-0.068858	0.88
8.4	-0.04095	-0.04101235	0.15
9.45	-0.0231	-0.02274725	-1.55
10.5	-0.01365	-0.013114	-0.17

By comparing the published coordinates with the generated coordinates, the percentage error reveals a error range of -3% to +1%

4.2 EXECUTION OF PHASE 2

4.2.1 Experimental Model Design Considering Ground Effect

Varied parameters

Assume the maximum fluid velocity is 200 km/h (A real Aircraft is reaching the maximum velocity of 200km/h during take off and landing).

Table 4.3: Boundary conditions

Parameter	Symbol	Range
Reynolds Nnumber	Re	0.1×10^6 to 0.4×10^6
Angle of Attack	α	-4^0 to 20^0
Height to Chord Ratio	H/C	0.1 to 1.0

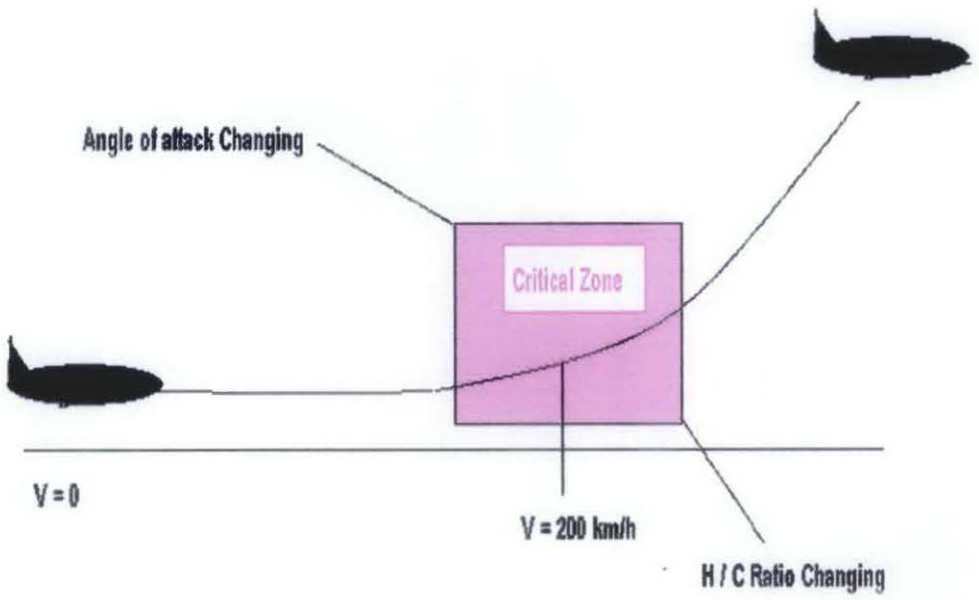

Figure 4.3: Critical Zone for Experimental Analysis

4.2.2 Wind Tunnel Experimental Arrangement

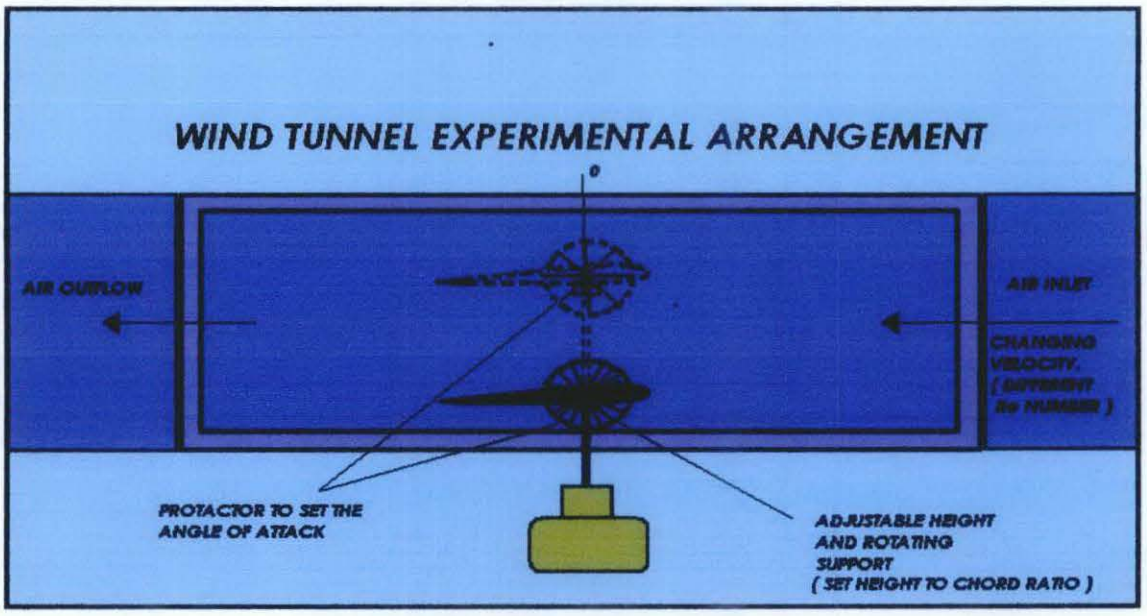

Figure 4.4: Experimental Arrangement

Figure 4.5: Subsonic Wind Tunnel

Figure 4.5 shows the subsonic wind tunnel used in this project to carry out the experiments using the Airfoil Model.

Figure 4.6 below shows the NACA 4412 Model manufactured by previous student [11]. The model is fabricated in fulfillment of the student's thesis. Thus this model is going to be used for the experimental analysis

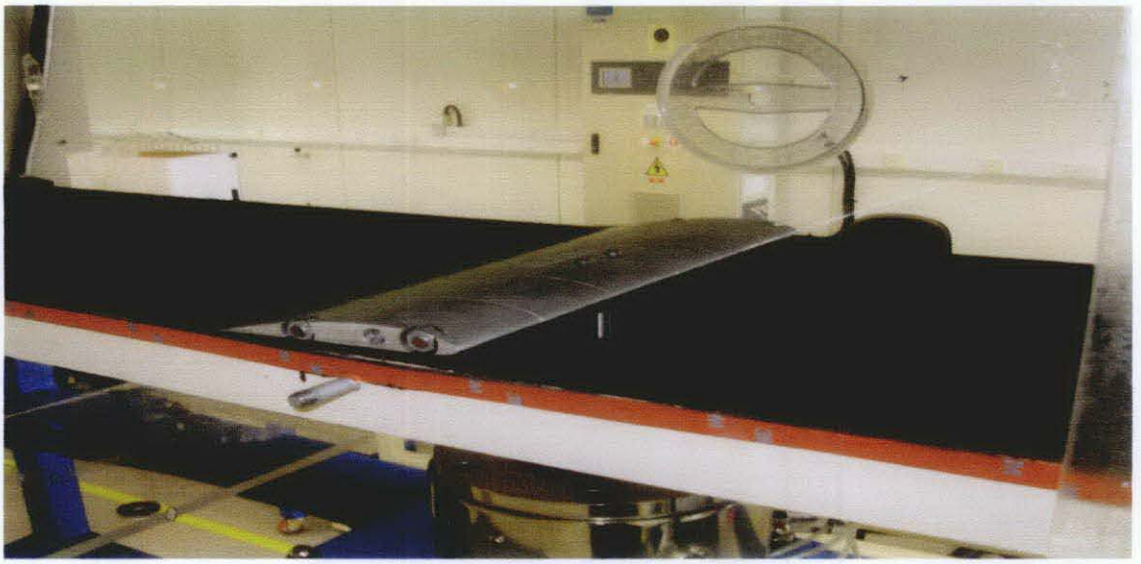

Figure 4.6: NACA 4412 Airfoil Model

Figure 4.7: Test section floor as ground

Figure 4.8 shows the arrangement of the airfoil inside the wind tunnel test section. The test section's floor is accounted as the ground for the experimental analysis

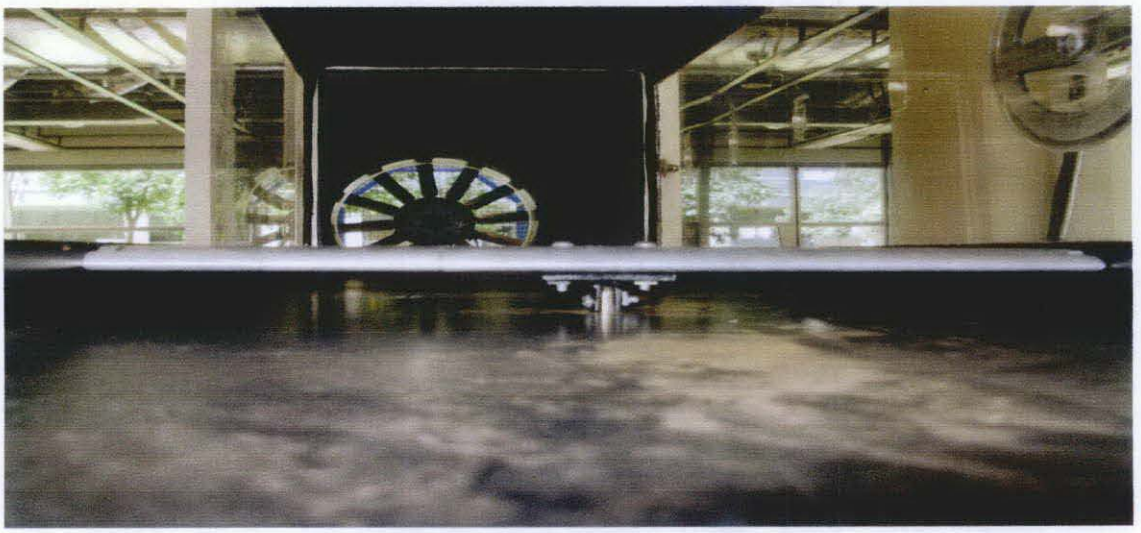

Figure 4.8: Sample arrangement of the airfoil closer to the ground

Figure shows a closer look of the airfoil model arrangement inside the test section. After setting the airfoil into the test section, the velocity was applied according to the Re number (0.1-0.4 x 10^6). For every range of velocity the data are gathered which are forces of lift, drag and pitching moment. The experiment is repeated for different angle of attack and for each height to chord ratio ranging from 0.1 to 1.0.

4.2.3 Experimental Results

For H/C = 0.1 and Re = 0.4 x 10^6

Table 4.4: Angle of Attack against Coefficient of Lift, Drag and Moment

H/C = 0.1, Re =0.4 e+6			
AOA	CL	CD	CM
-4	-4.67E-01	-7.03E-03	-4.92E+00
0	5.27E-03	6.27E-03	-3.09E+00
4	4.64E-01	1.29E-02	-3.62E+00
8	1.28E+00	1.32E-02	-2.09E+00
12	1.76E+00	2.98E-02	-1.44E+00
16	2.41E+00	3.73E-02	9.27E-02
20	2.06E+00	5.75E-02	1.62E+00

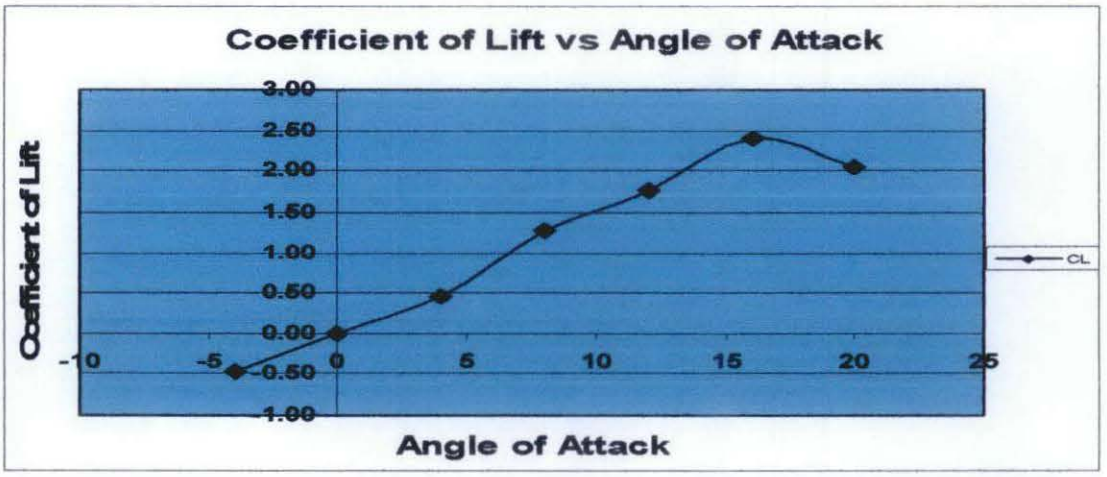

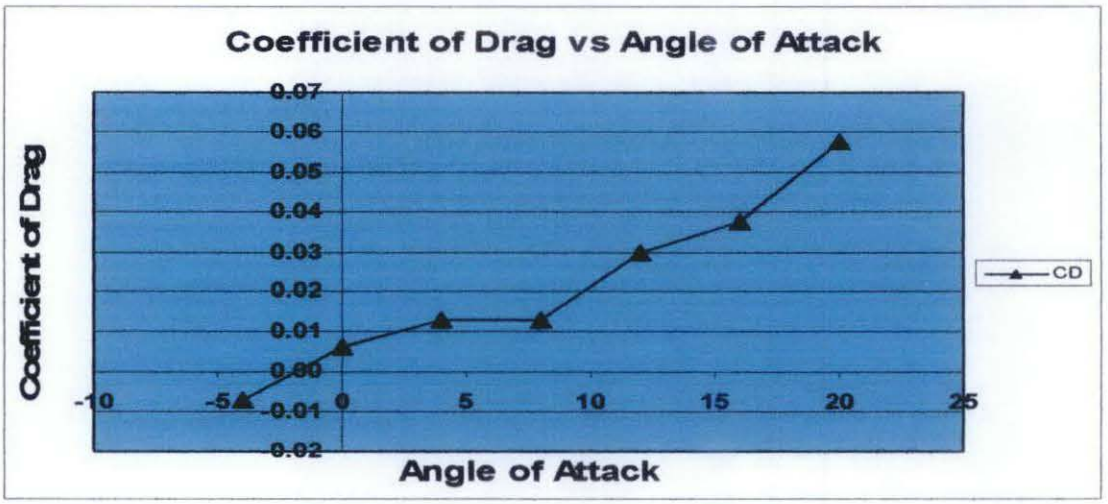

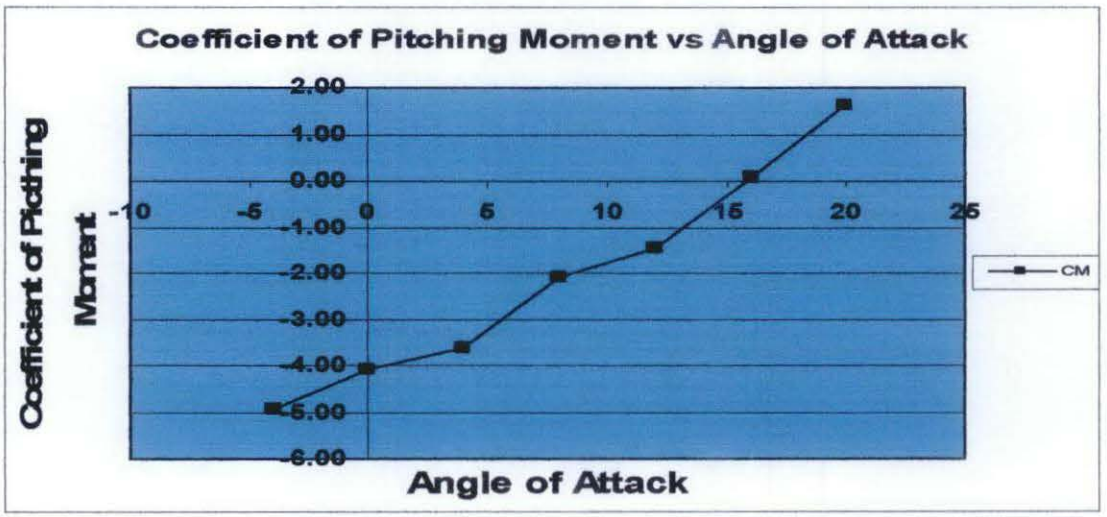

Figure 4.9: Graph of AOA against Coefficient of Lift, Drag and Moment

For H/C = 0.1, Angle of Attack = 4^0

Table 4.5: Reynolds Number against Coefficient of Lift, Drag and Moment

AOA = 4, H/C = 0.1			
Re	CL	CD	CM
4.00E+05	4.64E-01	1.29E-02	-6.22E-01
3.00E+05	3.21E-01	1.16E-02	-5.87E-01
2.00E+05	1.43E-01	7.52E-03	-2.62E-01
1.50E+05	8.05E-02	4.42E-03	-1.46E-01
1.00E+05	3.58E-02	2.15E-03	-6.57E-02

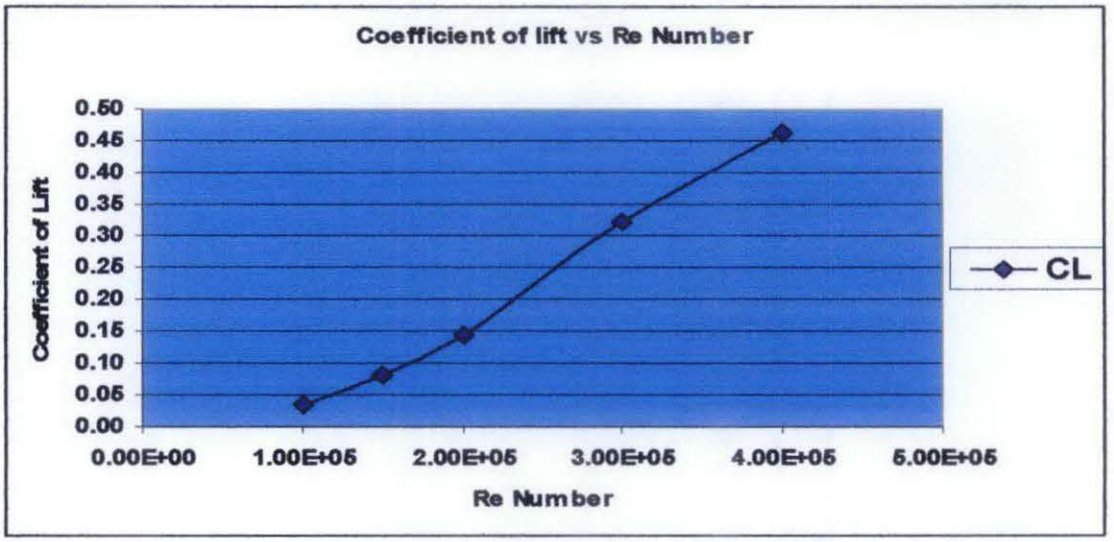

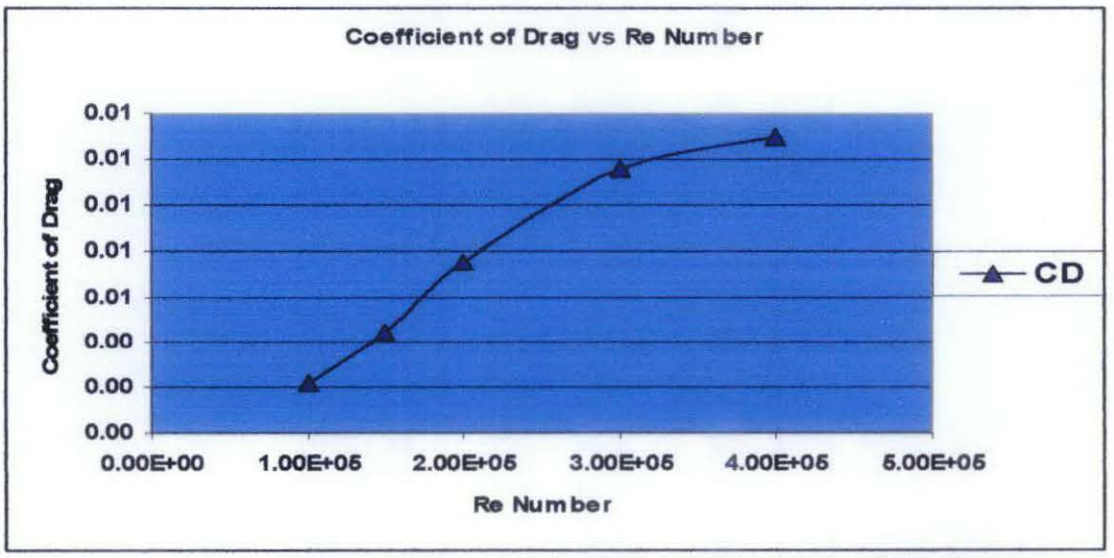

Figure 4.10: Graph of Re Number against Coefficient of Lift and Drag

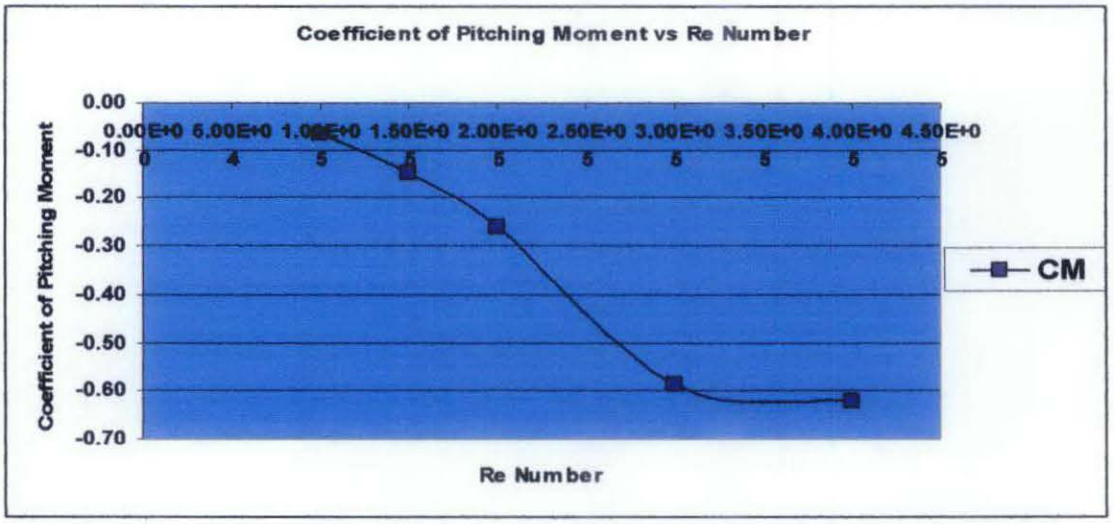

Figure 4.11: Graph of Re Number against Coefficient of Pitching Moment

For Re = 0.4 x 10^6 and Angle of Attack = 4^0, 8^0, 12^0

Table 4.6: Height to Chord Ratio against Coefficient of Lift and Drag

H/C	Coefficient of Lift		
	AOA = 4	AOA = 8	AOA = 12
0.1	1.17E+00	1.23E+00	1.37E+00
0.2	1.15E+00	1.21E+00	1.32E+00
0.4	1.14E+00	1.20E+00	1.28E+00
0.6	1.12E+00	1.19E+00	1.25E+00
0.8	1.10E+00	1.16E+00	1.24E+00
1	1.08E+00	1.14E+00	1.22E+00

H/C	Coefficient of Drag		
	AOA = 4	AOA = 8	AOA = 12
0.1	1.78E-02	1.49E-02	1.30E-02
0.2	1.61E-02	1.41E-02	1.19E-02
0.4	1.87E-02	1.44E-02	1.23E-02
0.6	1.88E-02	1.46E-02	1.25E-02
0.8	1.90E-02	1.50E-02	1.31E-02
1	1.91E-02	1.51E-02	1.33E-02

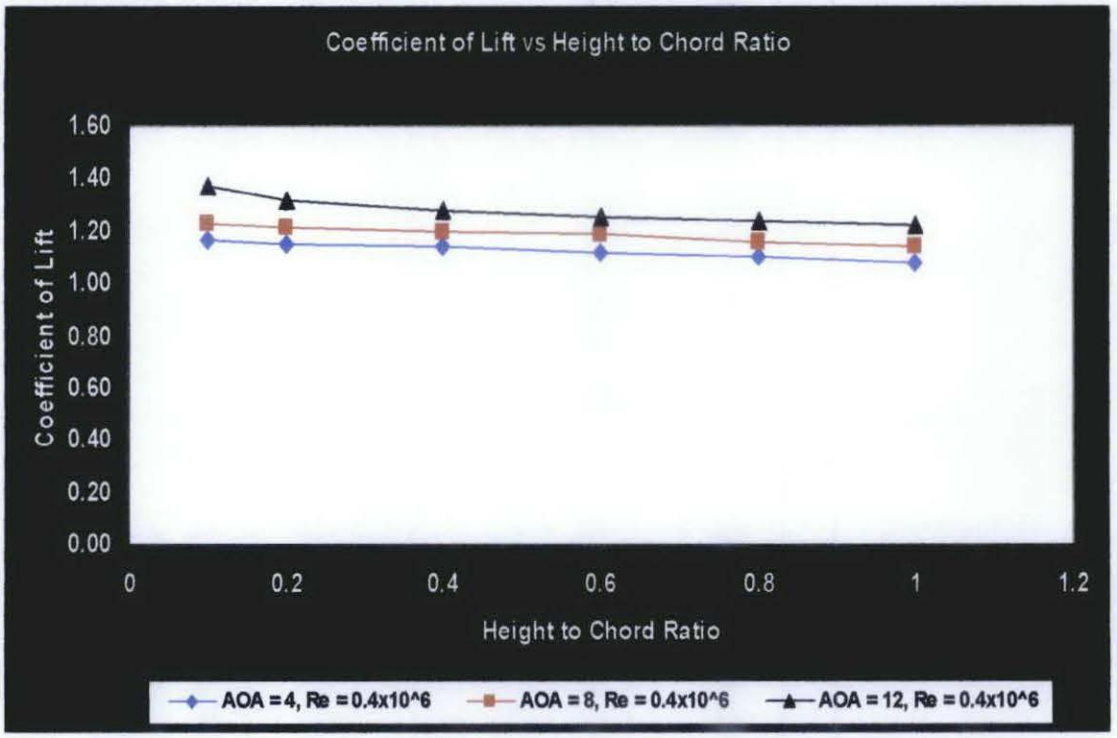

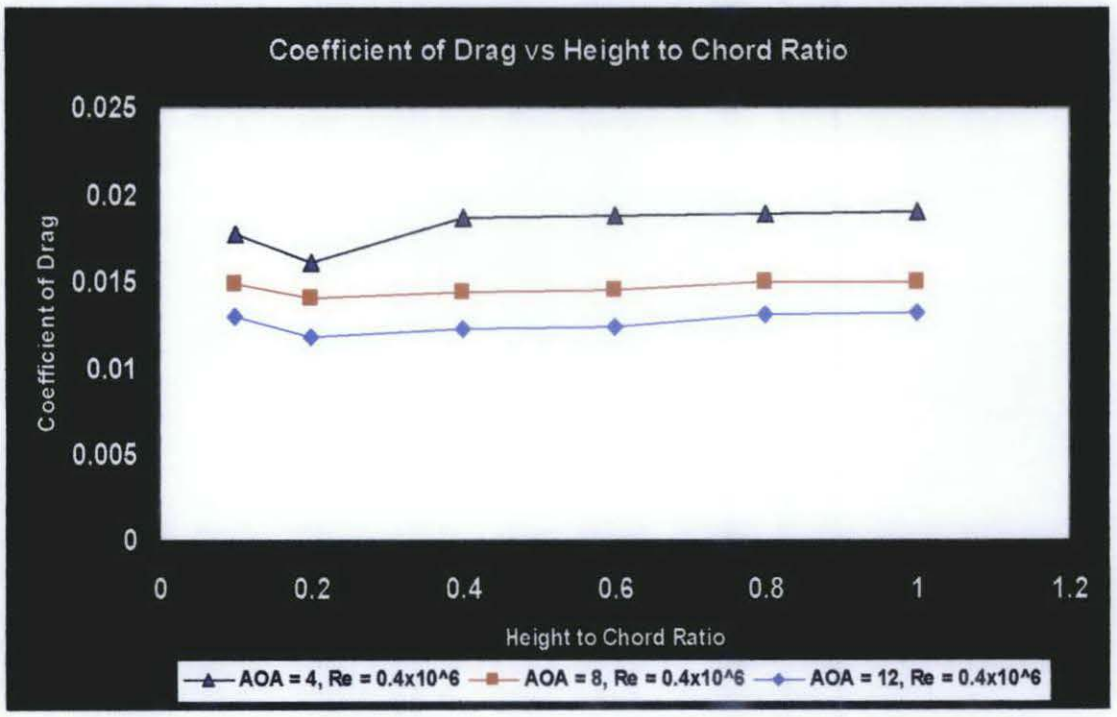

Figure 4.12: Graph of H/C Ratio against Coefficient of Lift and Drag

4.3 EXECUTION OF PHASE 3

4.3.1 Create the NACA 4412 Airfoil model using GAMBIT software.

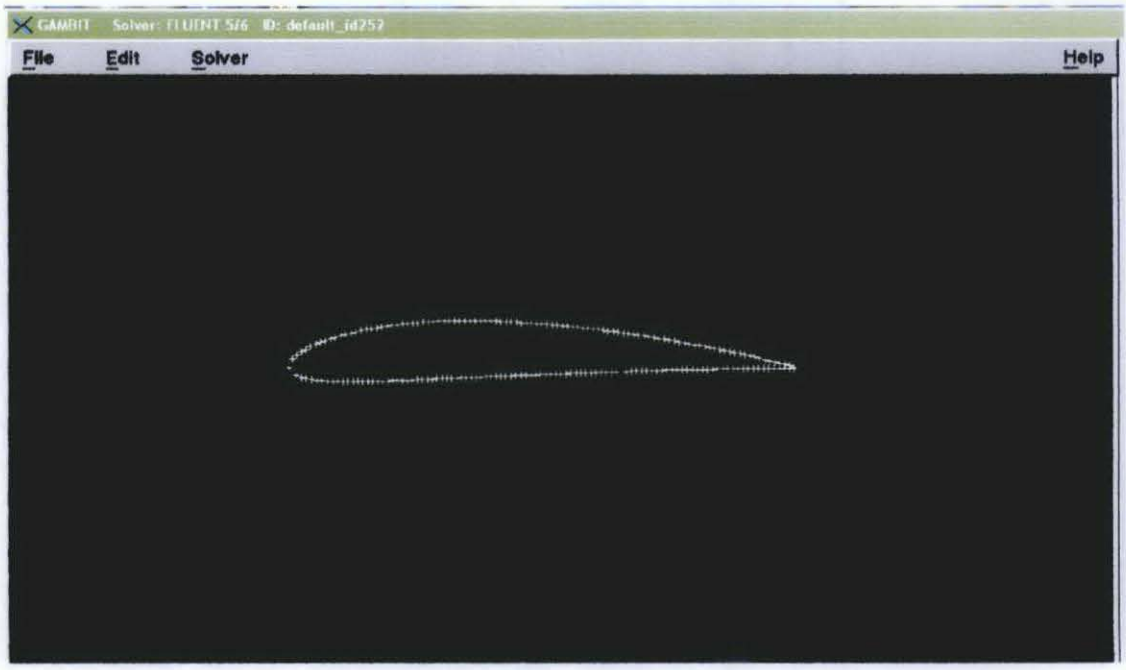

Figure 4.13: NACA 4412 Vertexes plotted on GAMBIT

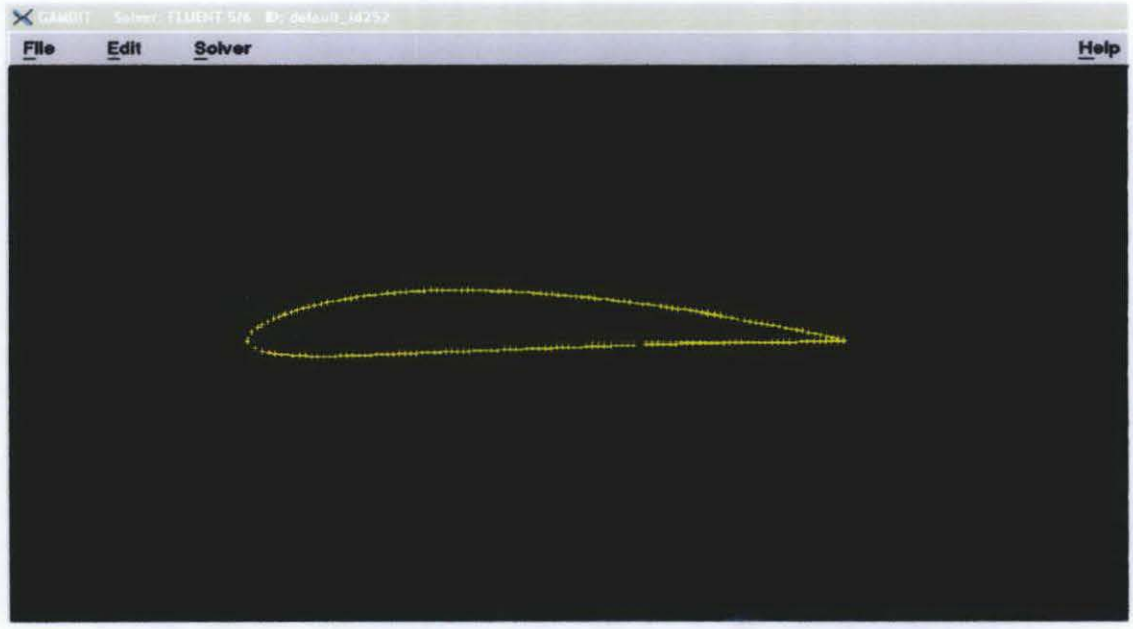

Figure 4.14: NACA 4412 Edges plotted on GAMBIT

4.3.2 Set the boundaries for ground effect analysis using GAMBIT.

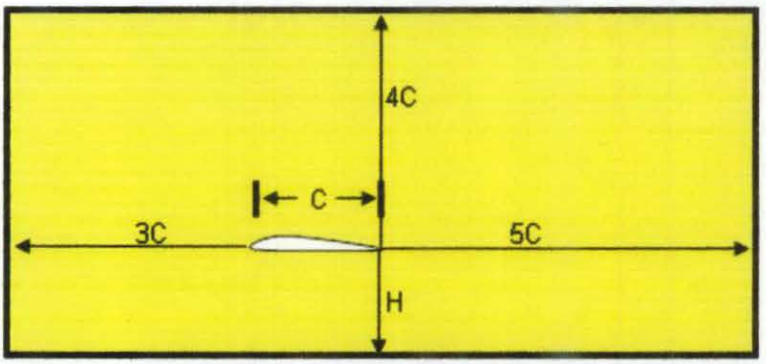

Figure 4.15: Boundary Model

Justification for the boundary selection

Height H

The height represents the distance of the Airfoil to the ground

Outflow 5C

The outflow region is selected to be at five times the chord length because the coefficient values of the drag, lift and pitching moment is unstable if the region is selected closer than five times the chord length. Further from 5C the values obtain are stable.

Velocity inlet 3C

The velocity inlet region is selected to be at three times the chord length because the coefficient values of the drag, lift and pitching moment is unstable if the region is selected closer than three times the chord length. Further from 3C the values obtain are stable.

Far flow 4C

The far flow region is selected to be at four times the chord length because it represents the empty surface above the airfoil. The values obtain below the 4C has the influence of the pressure on the airfoil. In order to avoid the influence the minimum height above the chord length should four times the chord length

Based on literature survey, H/C ratio is usually taken as a variable which varies from H/C ratio = 0.08 to H/C ratio =1.0, But the critical zone were the aerodynamic characteristics are dramatically changing is when H/C ratio<= 0.1.

In order to analyze the phenomena, lets vary the H/C ratio from 0.1 to 1.0, lets take the first case as H/C ratio = 0.1.

H/C = 0.1

H = C * 0.1 = 10.5 *0.1 = 1.05 cm

5C = 5 * 10.5 = 52.5 cm

4C = 4 * 10.5 = 42.0 cm

3C = 3 * 10.5 = 31.5 cm

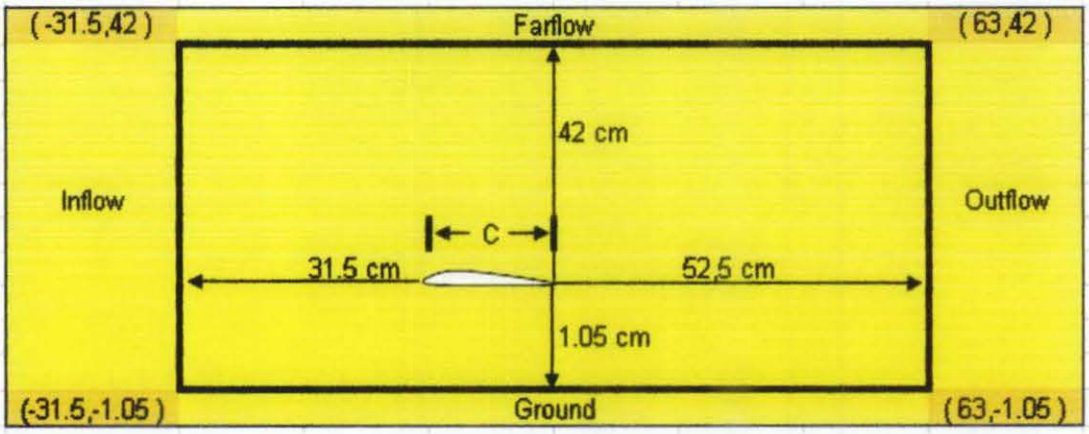

Figure 4.16: Boundary Model for H/C= 0.1 and angle of attack $\alpha = 0^{o}$

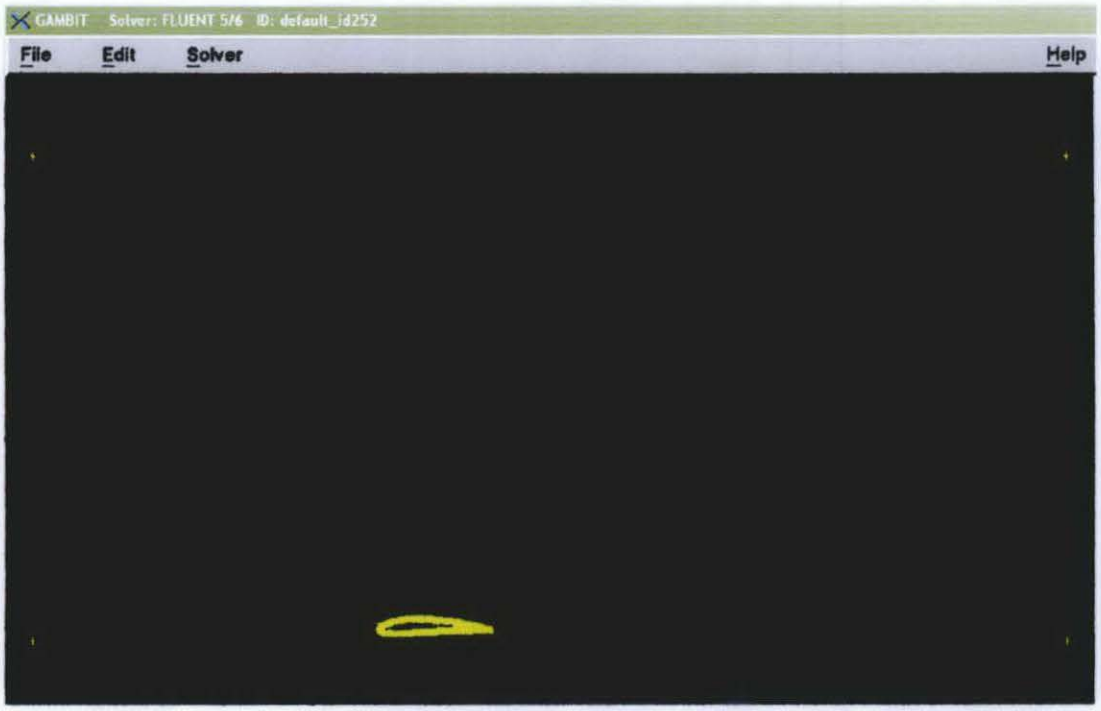

Figure 4.17: Boundaries applied in GAMBIT

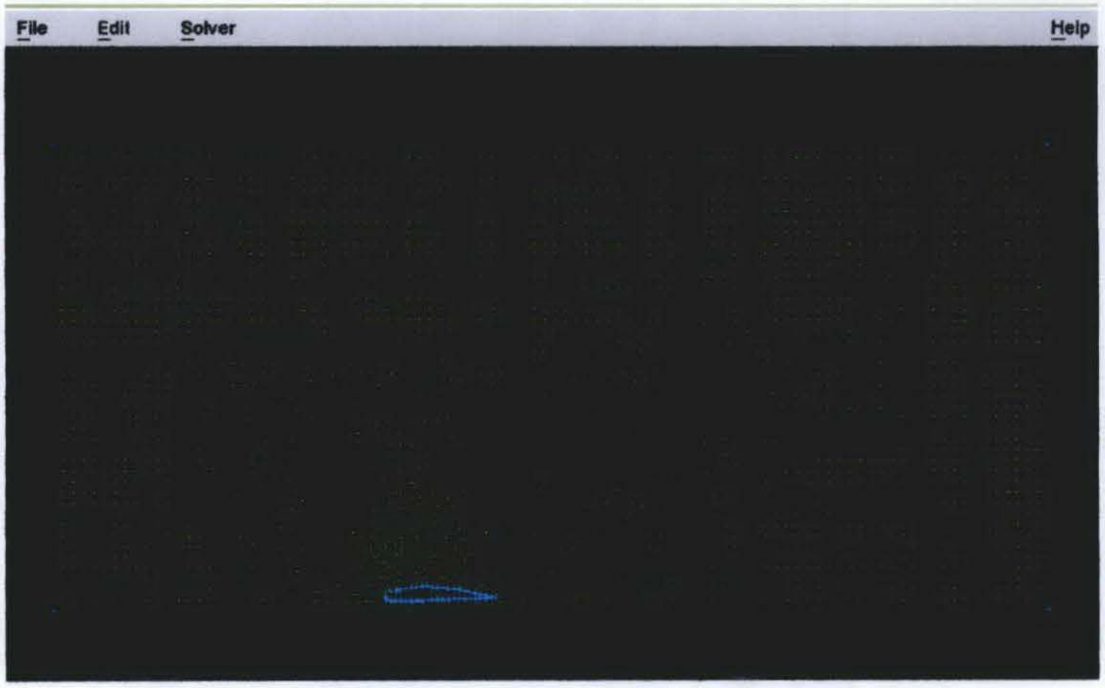

Figure 4.18: Stretched meshing of the flow field

4.3.3 FLUENT Analysis

Boundary Conditions

Flow over a 2D Airfoil (NACA 4412)

Reynolds Number = 0.1×10^6 to 0.4×10^6

Angle of Attack = -4^0 to 20^0

Height to Chord Ratio = 0.1 to 1.0

Table 4.7: Angle Of Attack

Angle of attack, α	Cos α	Sin α	x-velocity	y-velocity
-4^0	0.9976	-0.0698	45.888	-3.209
0^0	1	0	46	0
4^0	0.9976	0.0698	45.888	3.209
8^0	0.9903	0.1391	45.552	6.402
12^0	0.9781	0.2079	44.995	9.564
16^0	0.9613	0.2756	44.218	12.679
20^0	0.9397	0.342	43.226	15.733

Simulation Results

(H/C = 0.1, AOA =0^0, Re = 0.4×10^6)

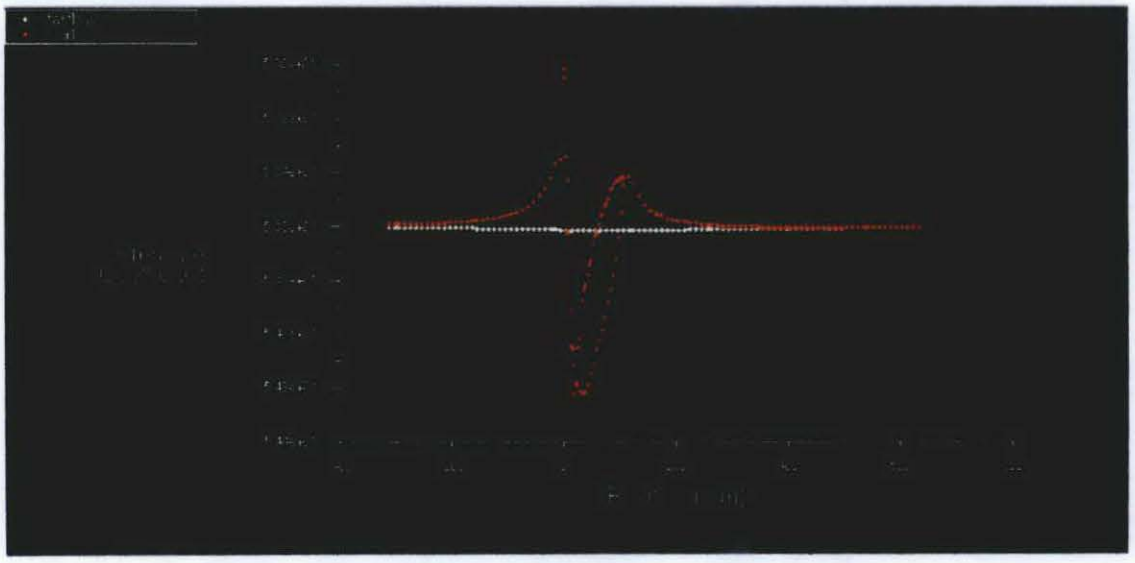

Figure 4.19: Pressure Coefficient against the position

Contour plots of the phenomena, as the airfoil approaches the ground

(H/C = 1.0, Re = 0.4 x 10^6)

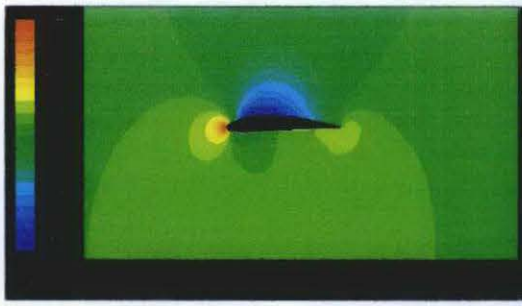

(H/C = 0.8, Re = 0.4 x 10^6)

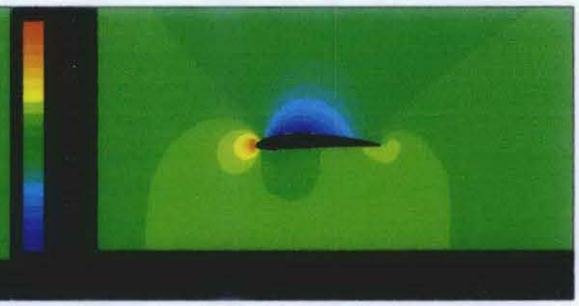

(H/C = 0.6, Re = 0.4 x 10^6)

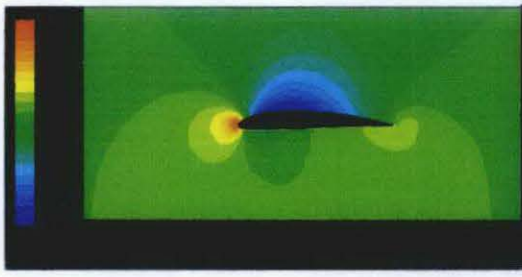

(H/C = 0.4, Re = 0.4 x 10^6)

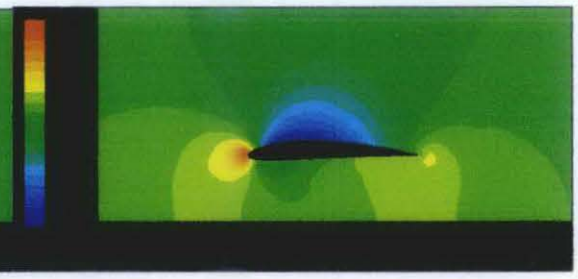

(H/C = 0.2, Re = 0.4 x 10^6)

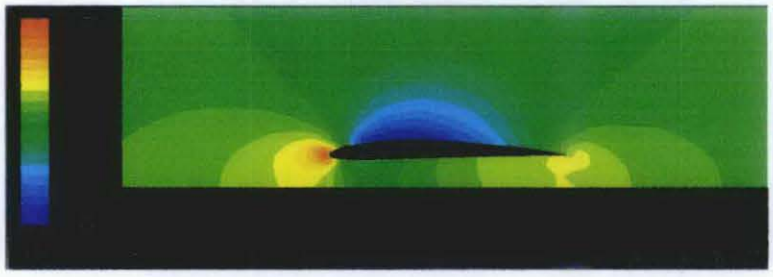

(H/C = 0.1, Re = 0.4 x 10^6)

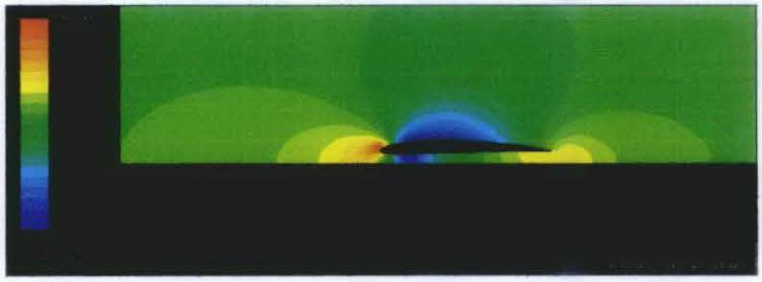

Figure 4.20: Contour of static pressure around the Airfoil

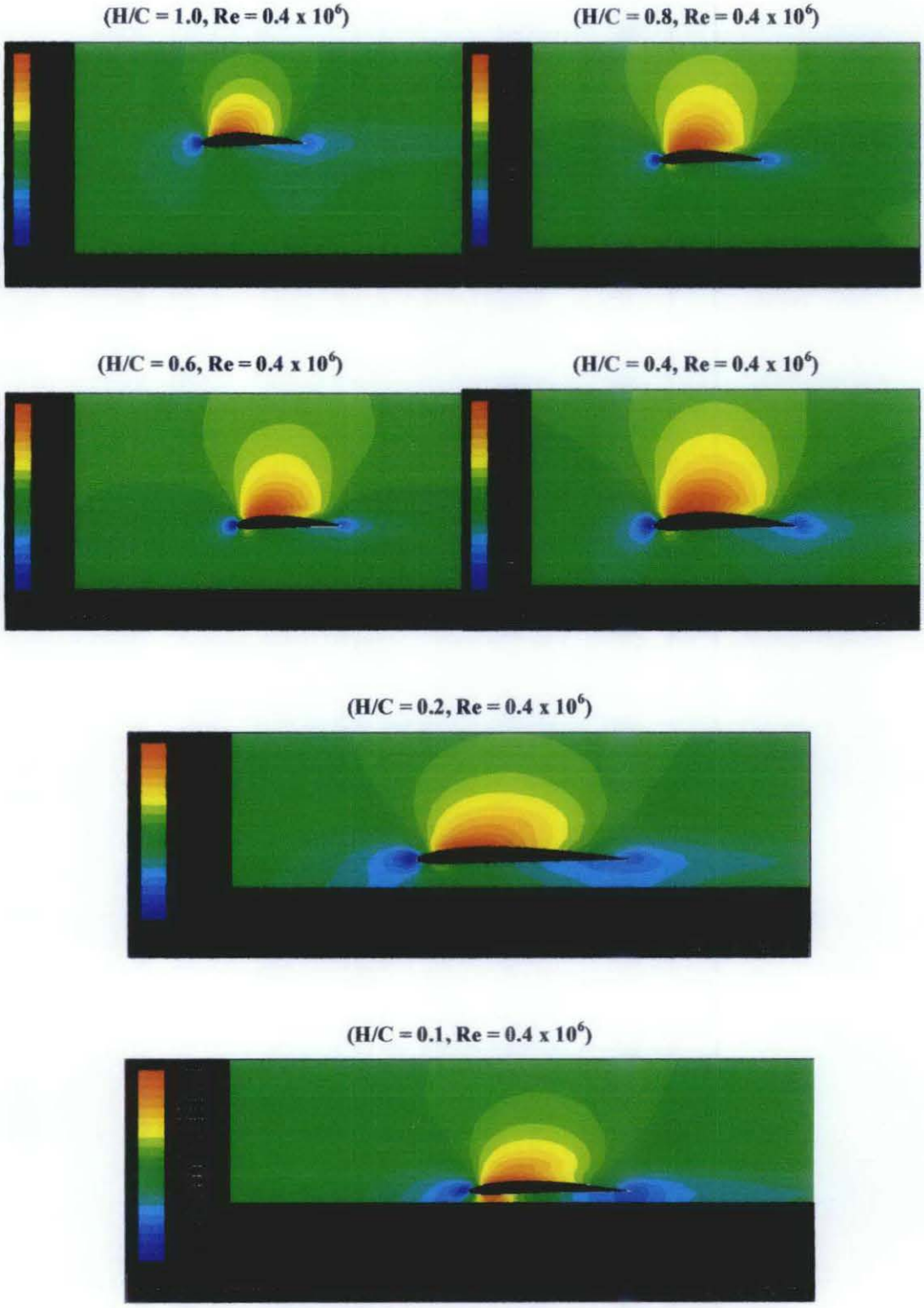

Figure 4.21: Contour of dynamic pressure around the Airfoil

(H/C = 1.0, Re = 0.4 x 10^6)

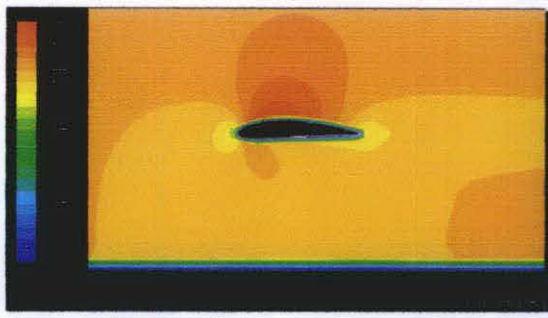

(H/C = 0.8, Re = 0.4 x 10^6)

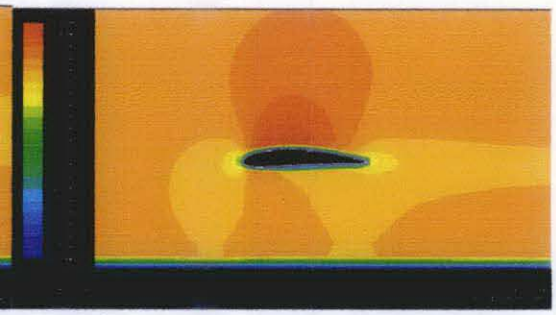

(H/C = 0.6, Re = 0.4 x 10^6)

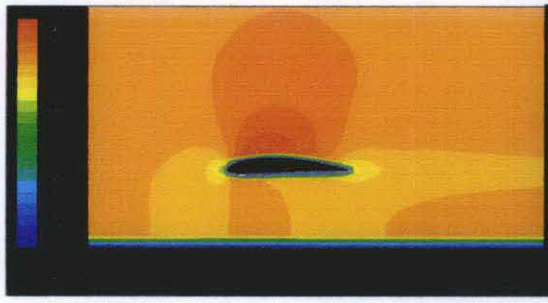

(H/C = 0.4, Re = 0.4 x 10^6)

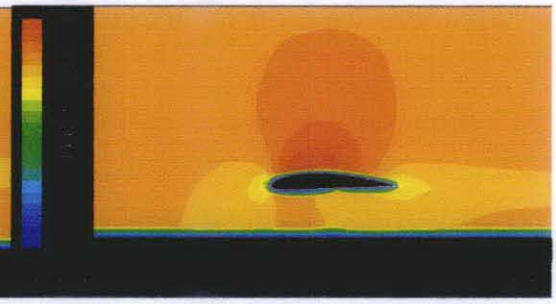

(H/C = 0.2, Re = 0.4 x 10^6)

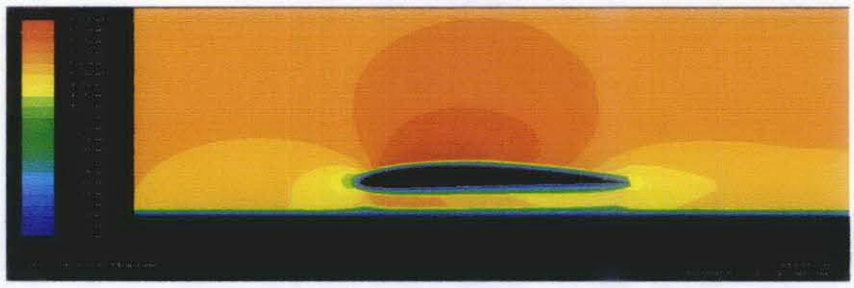

(H/C = 0.1, Re = 0.4 x 10^6)

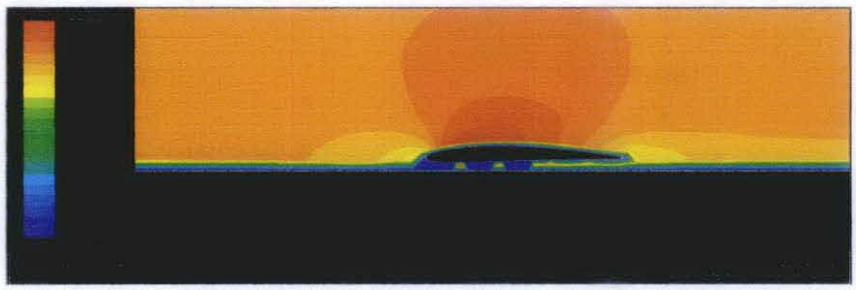

Figure 4.22: Contour of velocity magnitude around the Airfoil

The coefficients of Lift Drag and Pitching Moment

For H/C=0.1, Re = 0.4 x 10^6

Table 4.8: AOA against CL,CD, and CM

H/C = 0.1, Re =0.4 e+6			
AOA	CL	CD	CM
-4	-5.67E-01	-1.70E-03	-4.49E+00
0	4.18E-03	3.63E-03	-3.88E+00
4	5.71E-01	1.13E-02	-3.06E+00
8	1.13E+00	1.93E-02	-2.09E+00
12	1.68E+00	2.78E-02	-1.04E+00
16	2.68E+00	3.17E-02	5.93E-02
20	2.19E+00	4.57E-02	1.46E+00

AOA = Angle of Attack, **CL, CD, CM = Coefficient of lift, drag & moment**

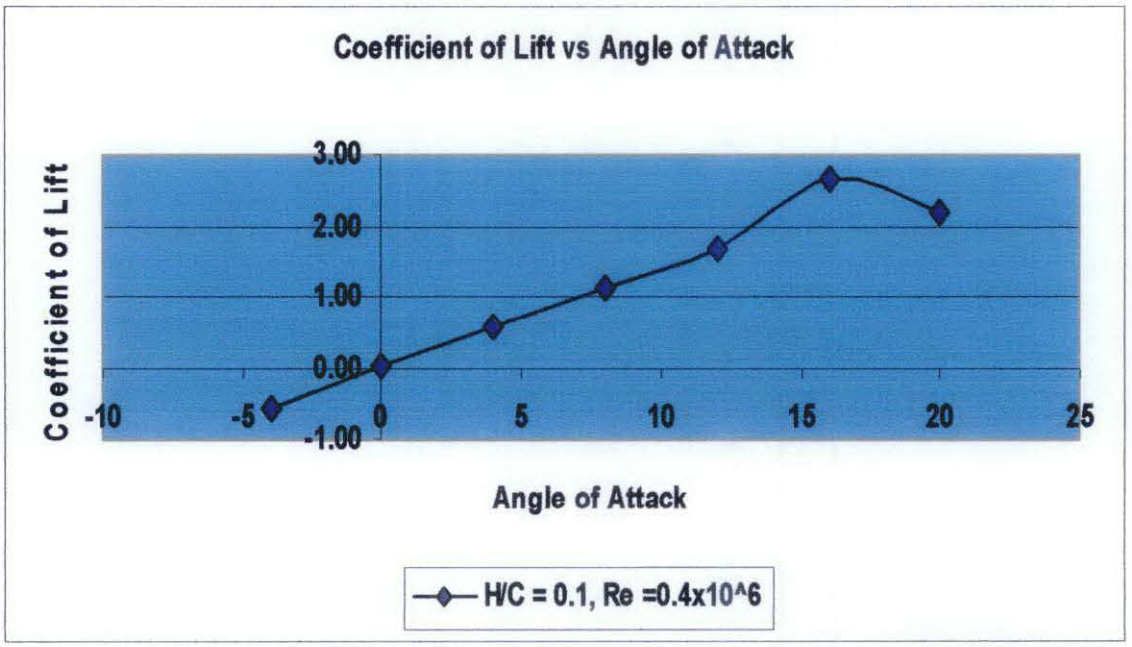

Figure 4.23: CL vs AOA at H/C = 0.1, Re =0.4 e+6

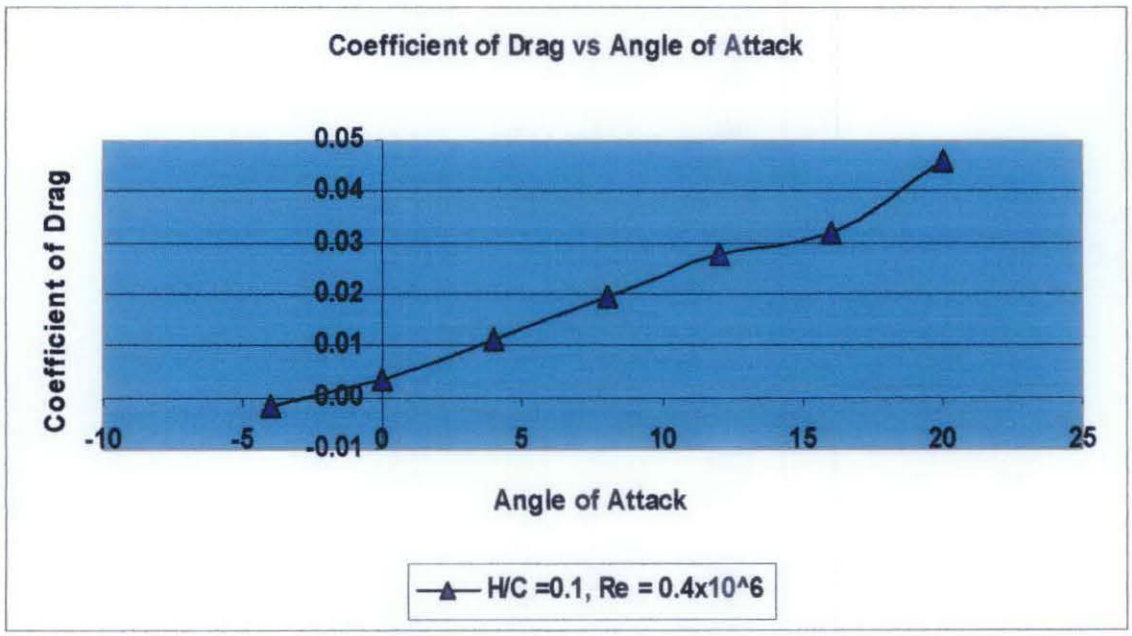

Figure 4.24: CD vs AOA at H/C = 0.1, Re =0.4 e+6

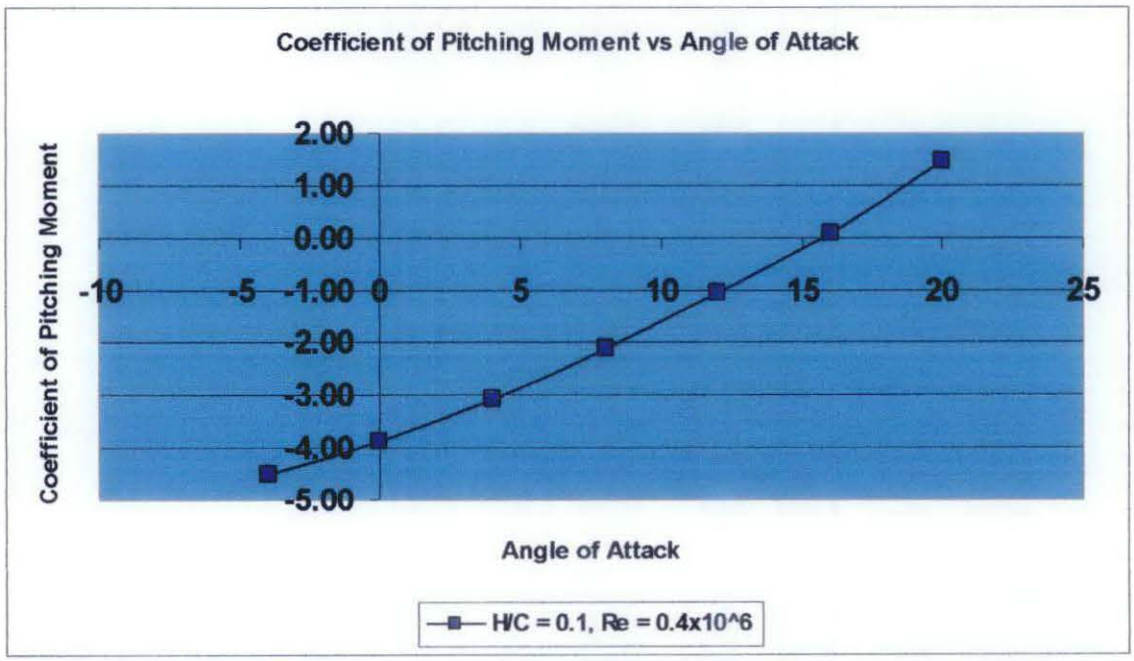

Figure 4.25: CM vs AOA at H/C = 0.1, Re =0.4 e+6

For H/C=0.1, AOA = 4^0

Table 4.9: Re against CL, CD, and CM

AOA = 4, H/C = 0.1			
Re	CL	CD	CM
4.00E+05	5.71E-04	2.78E-05	-1.04E-03
3.00E+05	3.21E-04	1.61E-05	-5.87E-04
2.00E+05	1.43E-04	7.52E-06	-2.62E-04
1.50E+05	8.05E-05	4.42E-06	-1.46E-04
1.00E+05	3.58E-05	2.15E-06	-6.57E-05

AOA = Angle of Attack, CL, CD, CM = Coefficient of lift, drag & moment

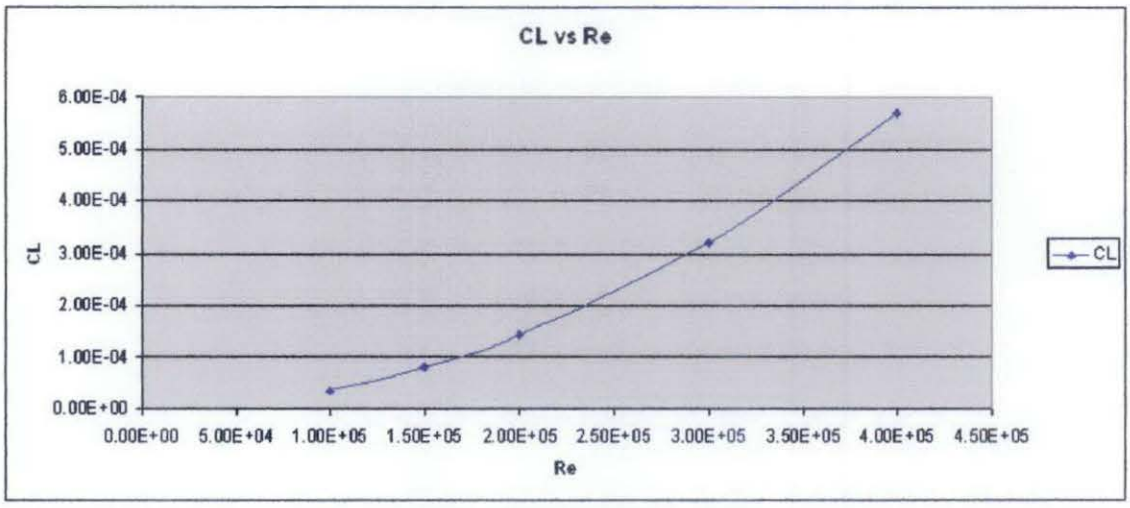

Figure 4.26: CL vs Re at AOA = 4, H/C = 0.1

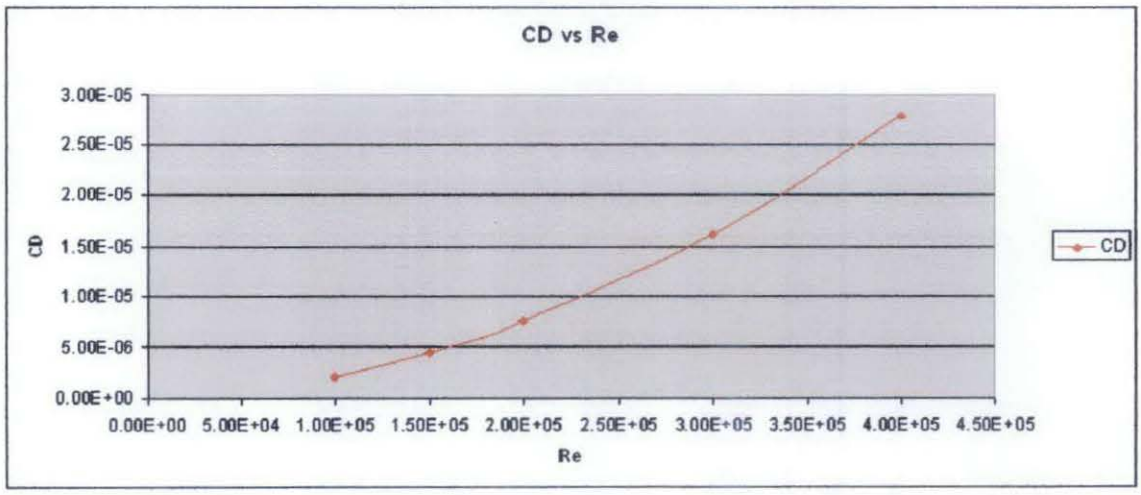

Figure 4.27: CD vs Re at AOA = 4, H/C = 0.1

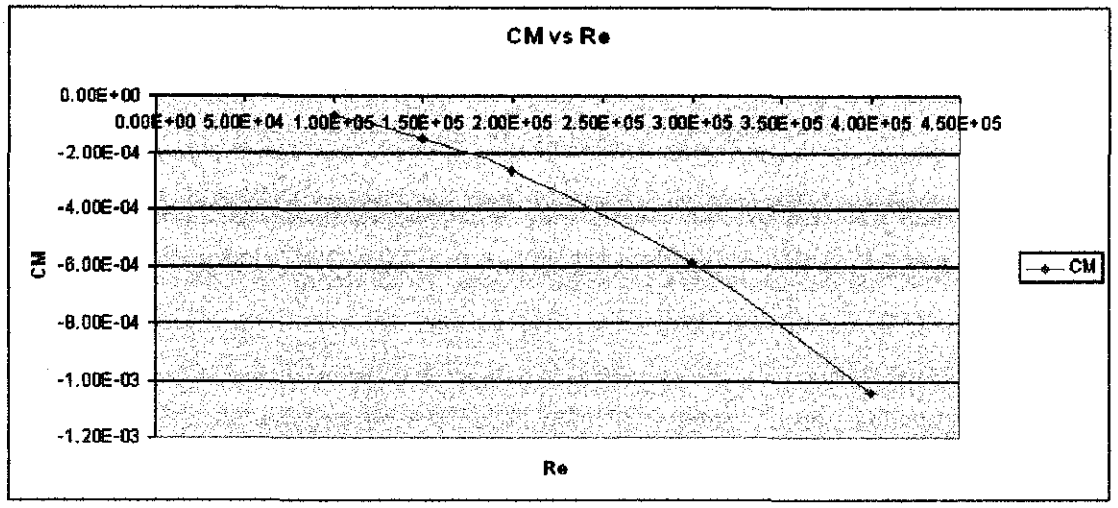

Figure 4.28: CM vs Re at AOA = 4, H/C = 0.1

For AOA = 4^0, 8^0,12^0 and Re = 0.4 x 10^6

Table 4.10: H/C Ratio against CL and CD

H/C	Coefficient of Lift		
	AOA = 4	AOA = 8	AOA = 12
0.1	5.71E-01	1.13E+00	1.67E+00
0.2	2.79E-01	9.56E-01	1.61E+00
0.4	2.73E-01	9.38E-01	1.57E+00
0.6	2.58E-01	9.11E-01	1.54E+00
0.8	2.46E-01	8.88E-01	1.51E+00
1	2.35E-01	8.69E-01	1.49E+00

H/C	Coefficient of Drag		
	AOA = 4	AOA = 8	AOA = 12
0.1	2.78E-02	3.93E-02	4.76E-02
0.2	1.87E-02	2.82E-02	3.72E-02
0.4	1.87E-02	2.82E-02	3.73E-02
0.6	1.88E-02	2.83E-02	3.74E-02
0.8	1.90E-02	2.86E-02	3.78E-02
1	2.41E-02	4.41E-02	5.55E-02

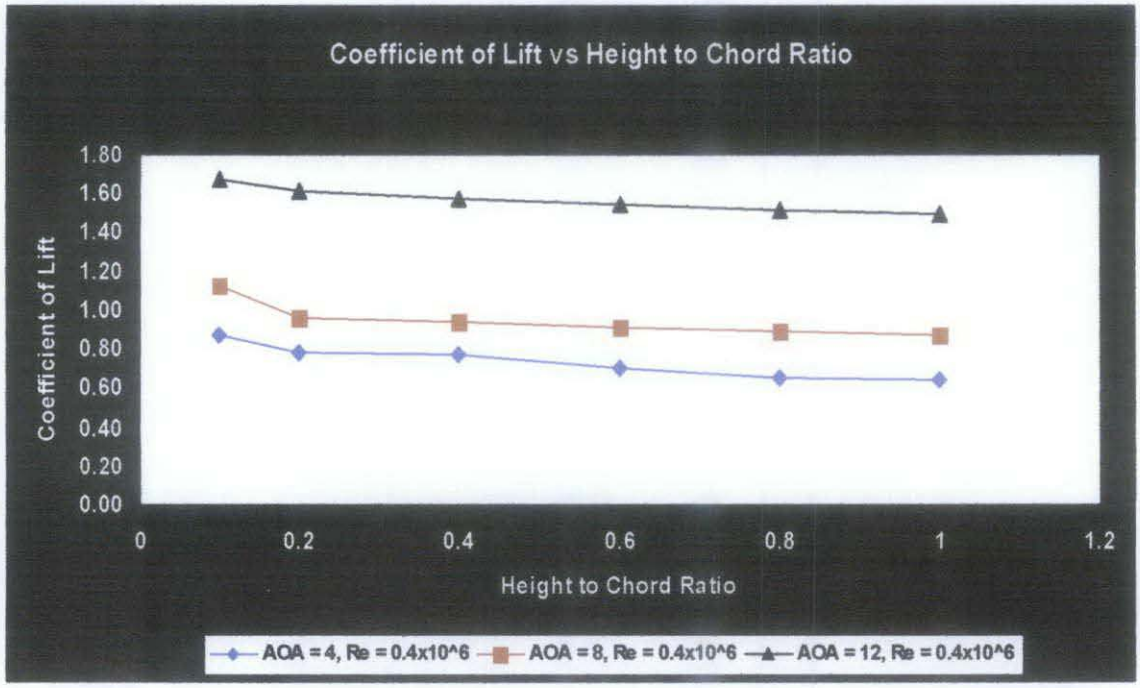

Figure 4.29: CL vs H/C Ratio at different Re and AOA

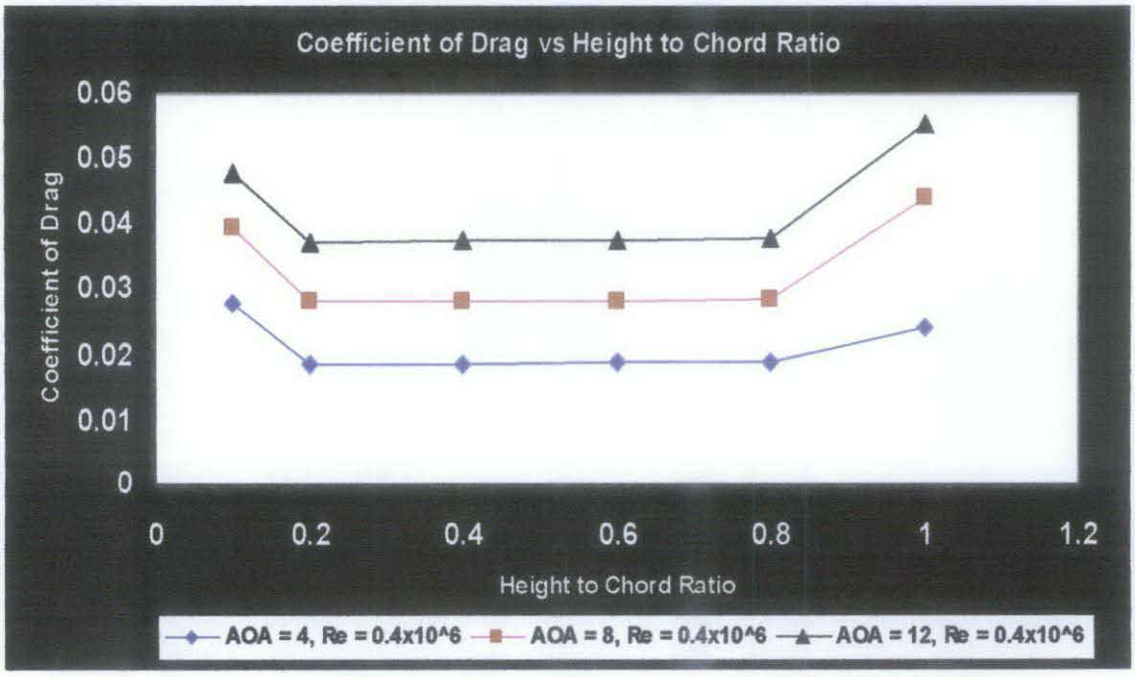

Figure 4.30: CD vs H/C Ratio at different Re and AOA

Comparison between Experimental and Numerical Results

Considering the plot of Coefficient of Lift and Drag against the Height to Chord Ratio.

For Re = 0.4 x10^6, and Angle of Attack = 4^0, 8^0, 12^0

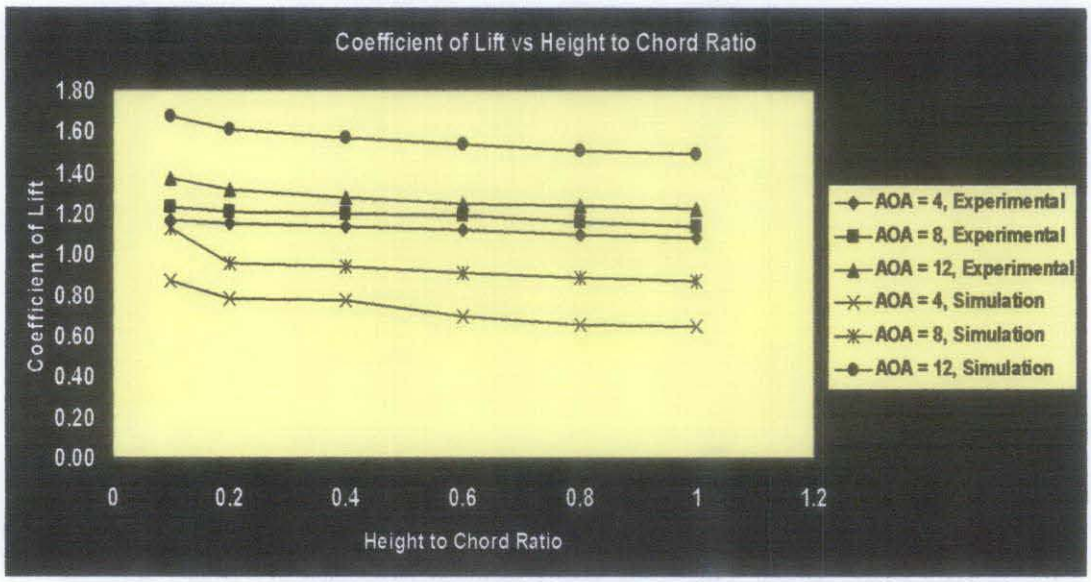

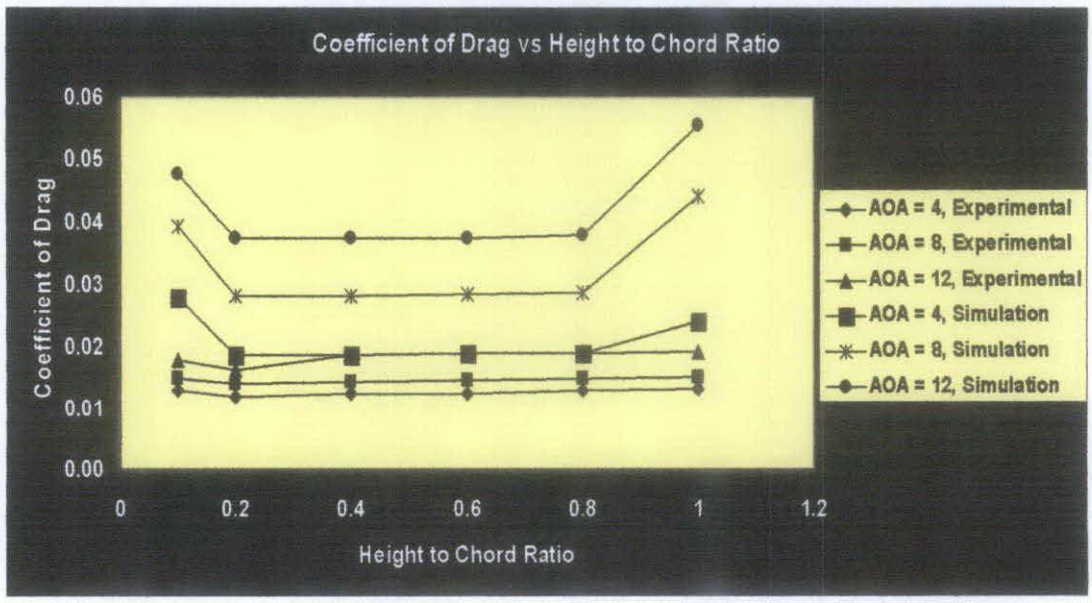

Figure 4.31: Comparison Graph of H/C Ratio against CL and CD

Percentage Error between the Experimental data and Simulation data obtained.

Table 4.11: Error between the Experimental data and Simulation data

Coefficient of Lift			
H/C	AOA = 4		
	Experimental	Simulation	% Error
0.1	1.17E+00	8.71E-01	25
0.2	1.15E+00	7.79E-01	32
0.4	1.14E+00	7.73E-01	32
0.6	1.12E+00	6.98E-01	37
0.8	1.10E+00	6.56E-01	40
1	1.08E+00	6.45E-01	40
H/C	AOA = 8		
	Experimental	Simulation	% Error
0.1	1.23E+00	1.13E+00	8
0.2	1.21E+00	9.56E-01	20
0.4	1.20E+00	9.38E-01	22
0.6	1.19E+00	9.11E-01	23
0.8	1.16E+00	8.88E-01	23
1	1.14E+00	8.69E-01	23
H/C	AOA =12		
	Experimental	Simulation	% Error
0.1	1.37E+00	1.67E+00	18
0.2	1.32E+00	1.61E+00	18
0.4	1.28E+00	1.57E+00	18
0.6	1.25E+00	1.54E+00	19
0.8	1.24E+00	1.51E+00	18
1	1.22E+00	1.49E+00	18

Coefficient of Drag			
H/C	AOA = 4		
	Experimental	Simulation	% Error
0.1	1.30E-02	2.78E-02	50
0.2	1.19E-02	1.87E-02	36
0.4	1.23E-02	1.87E-02	34
0.6	1.25E-02	1.88E-02	33
0.8	1.31E-02	1.90E-02	31
1	1.33E-02	2.41E-02	45
H/C	AOA = 8		
	Experimental	Simulation	% Error
0.1	1.49E-02	3.93E-02	60
0.2	1.41E-02	2.82E-02	50
0.4	1.44E-02	2.82E-02	50
0.6	1.46E-02	2.83E-02	50
0.8	1.50E-02	2.86E-02	50
1	1.51E-02	4.41E-02	65
H/C	AOA =12		
	Experimental	Simulation	% Error
0.1	1.78E-02	4.76E-02	62
0.2	1.61E-02	3.72E-02	56
0.4	1.87E-02	3.73E-02	50
0.6	1.88E-02	3.74E-02	50
0.8	1.90E-02	3.78E-02	50
1	1.91E-02	5.55E-02	65

The percentage error for coefficient of lift agrees within 40% error between experimental work and simulation work. For coefficient of Drag the value agrees within 60% error between experimental work and simulation work

Comparison between Experimental Work and Previous Work

Considering the plot of Coefficient of Lift and Drag against the Height to Chord Ratio.

For Re = 0.4 x10^6, and Angle of Attack = 4^0, 8^0

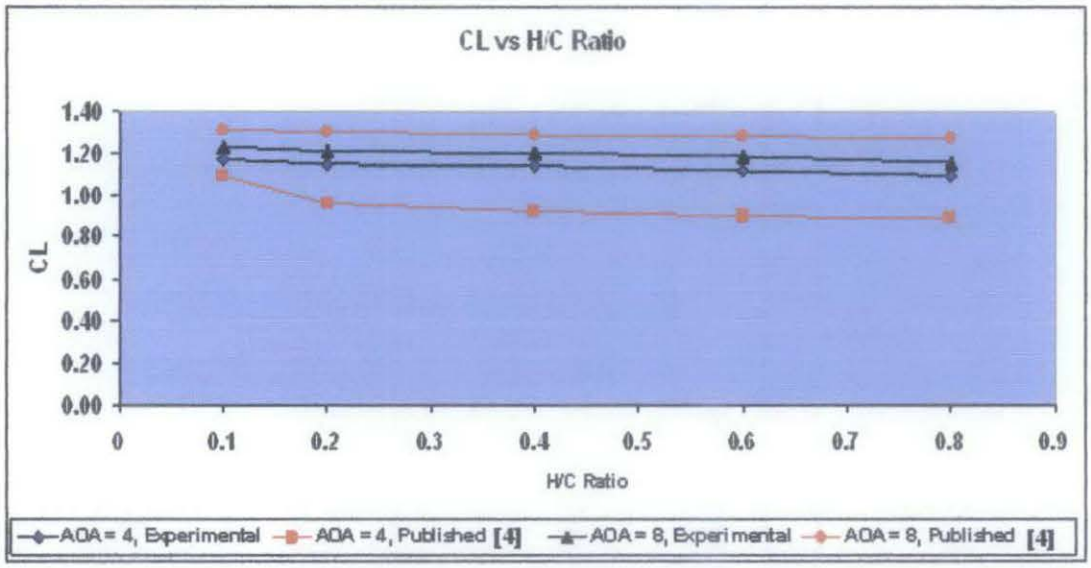

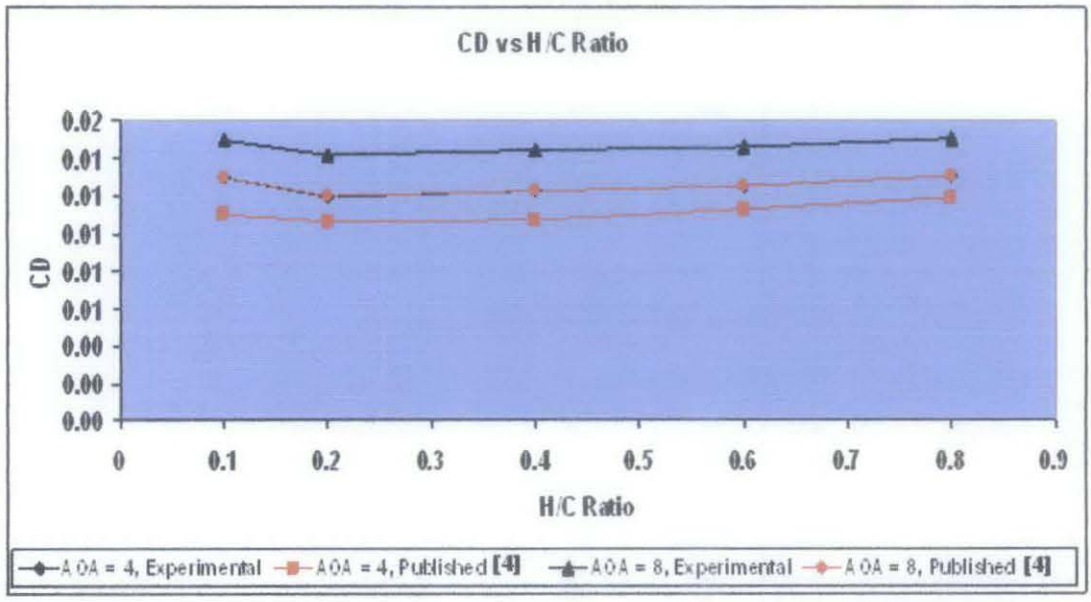

Figure 4.32: Comparison of Experimental work with previous work

Error estimation between Experimental work and previous work [4]

Table 4.12: Error between Experimental work and previous work

H/C	Coefficient of Lift					
	AOA = 4			AOA = 8		
	Experimental	Published [4]	% Error	Experimental	Published [4]	% Error
0.1	1.17E+00	1.1	6	1.23E+00	1.32	7
0.2	1.15E+00	0.96	16	1.21E+00	1.31	7
0.4	1.14E+00	0.92	20	1.20E+00	1.295	7
0.6	1.12E+00	0.9	20	1.19E+00	1.29	7
0.8	1.10E+00	0.89	20	1.16E+00	1.28	10

H/C	Coefficient of Drag					
	AOA = 4			AOA = 8		
	Experimental	Published [4]	% Error	Experimental	Published [4]	% Error
0.1	1.30E-02	0.011	15	1.49E-02	0.013	12
0.2	1.19E-02	0.0107	10	1.41E-02	0.012	15
0.4	1.23E-02	0.0108	12	1.44E-02	0.0123	15
0.6	1.25E-02	0.0113	10	1.46E-02	0.0125	15
0.8	1.31E-02	0.0119	9	1.50E-02	0.0131	12

The estimated lift coefficient value is within 20% error compared with the findings of Firooz and Gadami, 2006 [4]. While the drag coefficient is within 15% error compared with the same reference [4].

Comparison between Simulation Work and Previous Work

Considering the plot of Coefficient of Lift and Drag against the Height to Chord Ratio.

For Re = 0.4 x10^6, and Angle of Attack = 4^0, 8^0

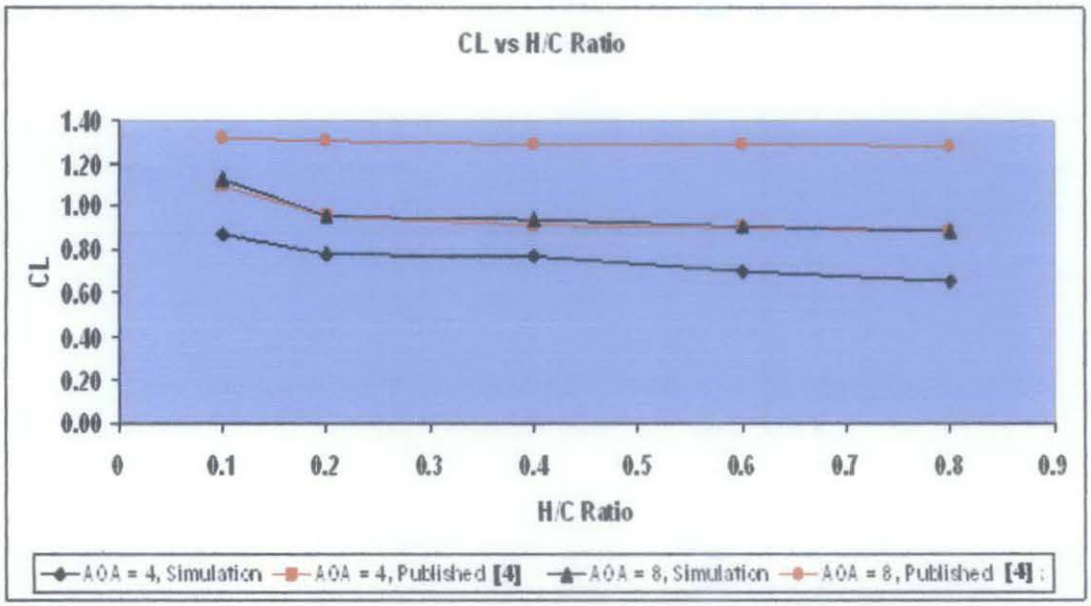

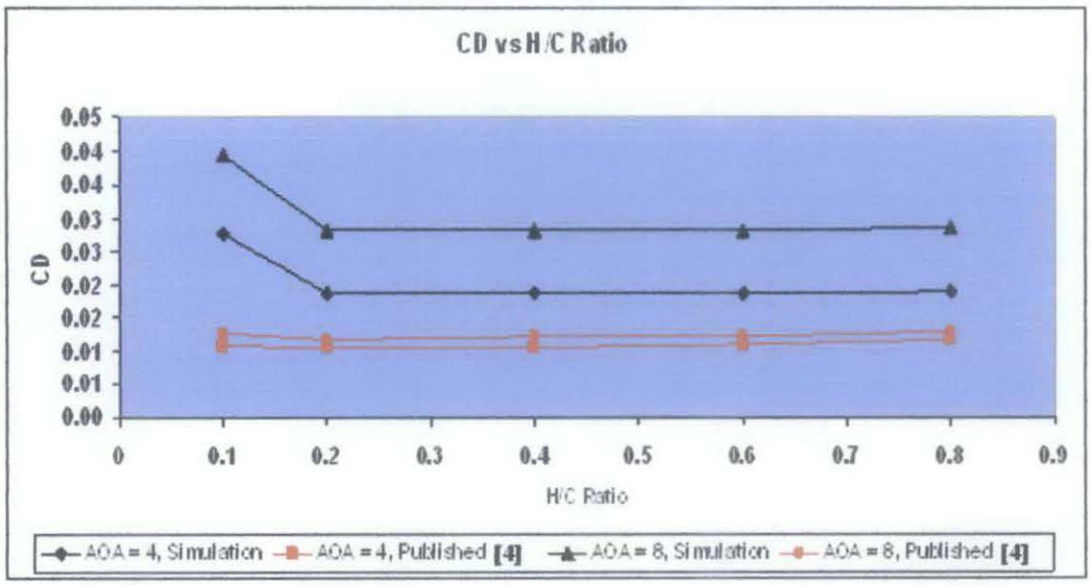

Figure 4.33: Comparison of Simulation work with previous work

Error estimation between Simulation work and previous work [4]

Table 4.13: Error between Simulation work and previous work

H/C	Coefficient of Lift					
	AOA = 4			AOA = 8		
	Simulation	Published [4]	% Error	Simulation	Published [4]	% Error
0.1	8.71E-01	1.1	20	1.13E+00	1.32	15
0.2	7.79E-01	0.96	18	9.56E-01	1.31	17
0.4	7.73E-01	0.92	16	9.38E-01	1.295	27
0.6	6.98E-01	0.9	22	9.11E-01	1.29	29
0.8	6.56E-01	0.89	26	8.88E-01	1.28	30

H/C	Coefficient of Drag					
	AOA = 4			AOA = 8		
	Simulation	Published [4]	% Error	Simulation	Published [4]	% Error
0.1	2.78E-02	0.011	60	3.93E-02	0.013	66
0.2	1.87E-02	0.0107	42	2.82E-02	0.012	57
0.4	1.87E-02	0.0108	42	2.82E-02	0.0123	56
0.6	1.88E-02	0.0113	40	2.83E-02	0.0125	55
0.8	1.90E-02	0.0119	37	2.86E-02	0.0131	54

The estimated lift coefficient value is within 30% error compared with the findings of Firooz and Gadami, 2006 [4]. While the drag coefficient is within 60% error compared with the same reference [4].

4.4 Discussion

As the airfoil approaches the ground, the pressure on the higher pressure side of the airfoil increases and end up with a large lift increase. Therefore on different angle of attack lift coefficient increases as it moves closer to the ground. The drag coefficient decreases far from ground and increases as it approaches the ground

Wing in Ground effect during take-off / landing is the cause of many aircraft accidents. A small plane loaded beyond gross weight capabilities may be able to take off under ground effect, due to the low stall speed. Once the aircraft climbs to a height at which wingtip vortices can form, the wings will stall, and the aircraft will suddenly descend and usually resulting in a crash.

These accidents occur because of lack of knowledge about aircraft performance. It happens because of inadequate pre-flight planning making allowances for the aircraft's performance limitations on the day of the accident. Accident reports of an apparent sudden and unexplained reduction of thrust soon after rotation on takeoff and aircraft floating off the end of a strip during landing. Pilots killing themselves when they lose control of an aircraft during the takeoff phase of flight. [13]

Lack of understanding of the relationship between lift, drag and ground effect is a contributory factor in many of these incidents and accidents.

In order to bring solution to the problem the manufacturer of the aircraft has to take the ground effect into consideration to produce the best design that will able to overcome the collision phenomena. On the other hand the pilots has to be well trained and aware about the wing in ground effect during take off and landing to handle the situation

CHAPTER 5
CONCLUSION

5.1 CONCLUSION

As a conclusion, the objective of the work has been achieved. The execution plan for the project has been carried out in three phase.

Phase 1: NACA 4412 profile identification
Phase 2: Experimental analysis was conducted
Phase 3: CFD simulation work was conducted

The coordinates are obtained using CNC Laser digitizer and the data were compared with published data. The Airfoil section has been modeled experimentally and tested in a subsonic wind tunnel under various operational conditions to study the interference near the ground. The case has been successfully simulated using CFD simulation (GAMBIT and FLUENT). The Airfoil characteristics have been obtained from the Experimental work and CFD simulation. The results were compared between the experimental work and simulation work. Besides that, partial of the experimental and simulation results were compared to a previous work.

5.2 RECOMMENDATION

For the experimental work, by avoiding the method of pin the model to the test section, the surface of the airfoil can be smoother and better results can be obtain The vibration occur due to the slip condition between the airfoil and the test section has to be reduce in order to decrease the fluctuation of the data for more precise results.

For the simulation to obtain better results the number of coordinates of the airfoil can be increased to have smoother surface for analysis. Besides that we can improve the boundary condition by having a wider range of angle of attack, Reynolds number and the height to chord ratio to have better results.

Based on the theory, the analysis of ground effect can be done using the span to chord ratio replacing the height to chord ratio. This approach can be a good comparison of the results

REFERENCES

[1] Andy J. Keane and Prasanth B. Nair, 2005, Computational Approaches for Aerospace Design: The Persuit of Excellence, England, John Wiley & Sons Ltd.

[2] R.H. Barnard and D.R. Philphot, 1995, Aircraft Flight, England, Prentice Hall.

[3] Zhang and Jonathan, 2000, Experimental and Numerical analysis on Turbulent Wake behind a Single Element Wing in Ground Effect: Department of Aeronautics and Astronautics, School of Engineering Sciences, University of Southampton, England.

[4] A. Firooz, M. Gadami, 2006, Turbulence Flow for NACA 4412 in Unbounded Flow and Ground Effect with Different Turbulence Models and Two Ground Conditions: Mechanical Engineering Department, University of Sistan & Baloochestan, Iran.

[5] Nathan Logsdon, 2006, A Procedure for Numerically analyzing Airfoils and Wing Sections: The Faculty of the Department of Mechanical & Aerospace Engineering University of Missouri, Columbia.

[6] David Heffley, 2007, Aerodynamic Characteristics of a NACA 4412 Airfoil: Baylor University.

[7] www.aerospaceweb.org

[8] www.aerospaceweb.org/wingtip

[9] Yunus A.Cengel and John M. Cimbala, 2006, Fluid Mechanics, International Edition, McGraw Hill

[10] Ira H. Abbott, Albert E. Von Doenhoff, 1959, Theory of Wing Sections, Dover Publications Inc. New York

[11] Mohd Nuh Aizat Mohd Daut, 2008, CNC Manufacturing of NACA 4412 Wing Sections For Wind Tunnel Test, Dissertation from Mechanical Engineering Department of University of Technology PETRONAS.

[12] Ahmad khairuddin Bin Ahmad Kamal, 2008, CFD Simulation and Wind Tunnel Test of NACA 4412 Airfoil Wing Section at Different Angles of Attack, Dissertation from Mechanical Engineering, Department of University of Technology PETRONAS.

[13] www.gremline.com/index_files/page0023.htm

APPENDICES

APPENDIX A – SYMMETRIC/ASYMMETRIC AIRFOIL MODELS

Symmetric Cases	**NACA 0006, NACA 0009, NACA 0012, NACA 0018, NACA 0024, NACA 0030**
Asymmetric Cases	**NACA 2409, NACA 4409, NACA 6309, NACA 6409, NACA 6609, NACA 8409**
	NACA 2412, NACA 4412, NACA 6412, NACA 8312, NACA 8412, NACA 8612

Figure A1: Airfoil Models

APPENDIX B - FUNDAMENTAL FLUID MECHANICS

The physical aspects of any fluid flow are governed by the 3 fundamental principles of mechanics:

1) Conservation of Mass
2) Conservation of Momentum
3) Conservation of Energy

When expressed in terms mathematical equations, the governing equations for fluid (the Navier-Stoke's equations) takes the form of the respective partial differential equations. When the condition of incompressible flow is applied, the following sets of incompressible Navier-Stoke's equation are obtained: [5]

$$\nabla \bullet \mathbf{u} = 0 \qquad \text{-(B.1)}$$

$$\frac{\delta \mathbf{u}}{\delta t} + (\mathbf{u} \bullet \nabla) \bullet \mathbf{u} = -\frac{1}{\rho} \nabla \bullet \mathbf{p} + \nu \nabla^2 \mathbf{u} \qquad \text{-(B.2)}$$

$$\frac{\delta T}{\delta t} + (\mathbf{u} \bullet \nabla) \bullet T = \frac{k}{\rho c_p} \nabla^2 T \qquad \text{-(B.3)}$$

Reynolds number is qualitatively defined as the ratio of inertia force over viscous force and can be easily proven by the following.

Considering that the inertia force will follow the magnitude of the order ρU^2 and the viscous force is result from the shear stress. [5]

$$\tau = \mu \frac{\partial u}{\partial y} \approx \mu \frac{U}{L}$$

Hence by taking the ratio between the two:

$$\frac{\text{Inertia}}{\text{Viscous}} = \frac{\rho U^2}{\mu U / L} = \frac{\rho U L}{\mu}$$